Acid−Base Hydrolytic Chemistry Route to Thin Films Containing Terminal Donor Ligands and Organometallic Complexes for Heterogenization of Metal Complex Catalysis

Maria G. L. Petrucci and Ashok K. Kakkar*

Department of Chemistry, McGill University, 801 Sherbrooke Street West, Montreal, Quebec H3A 2K6, Canada

A general synthetic approach based on the hydrolysis of R'_3Si-NR_2 with organic compounds containing acidic protons, to construct thin films of donor ligands on inorganic oxide surfaces that are subsequently used to support a variety of organometallic complexes, is reported. The reaction of surface hydroxyl groups on silica, glass, quartz, and single-crystal silicon with $SiCl_4$, followed by NEt_2H, affords surface-anchored $Si-NEt_2$ moieties which, upon simple acid−base hydrolysis with $HO-(CH_2)_n-XR_2$ ($n = 3$, $X = N$, $R = C_2H_5$; $n = 3$, $X = P$, $R = C_6H_5$; $n = 4$, $X = P$, $R = C_2H_5$), $HO-C_6H_4-XR_2$ ($X = P$, $R = C_6H_5$; $X = N$, $R = C_2H_5$), and $HO-CH(CH_3)-(CH_2)_3-N(C_2H_5)_2$ at ambient temperature, yield thin films containing terminal phosphine and amine donor ligands. These ligands are then used to covalently anchor organometallic complexes of Ni(0), Rh(I), Ru(II), and Pd(0) via bridge-splitting or ligand-displacement reactions. The synthesis of solution models to the surface-bound species and the characterization of the latter using numerous surface analytical techniques have proven useful in determining the conditions for the deposition process and in the evaluation of the structure of the supported metal complexes. A thin film of $[Si]-O-(CH_2)_3PPh_2Ni-(CO)_2PPh_3$ on glass catalyzes the oligomerization of phenylacetylene resulting in a product distribution different from that of a similar reaction in solution. The enhanced activity and selectivity of the organometallic Ni(0) thin films suggests that a positive role is played by the orientation of the surface-bound organometallic species in catalysis.

Introduction

The study of supported transition-metal complexes continues to attract widespread interest. The immobilization of transition-metal catalysts on solid supports has been shown to possess numerous advantages, including the ease of separation of the catalyst from the reaction products, and is expected to enhance catalytic activity and selectivity over their homogeneous counterparts.[1] From an industrial viewpoint, supported metal catalysis offers potential for the design of efficient catalytic systems with an advantageous combination of specific properties of homogeneous and heterogeneous phases.[2] Silica is a commonly employed anchor for heterogenizing homogeneous catalysis, since its surface hydroxyl groups offer rich chemistry[3] to covalently attach donor ligands which can then be used to introduce transition-metal complexes. The traditional syn-

thetic routes for the preparation of thin films containing donor ligands utilize the weakly acidic surface of silica, which permits condensation reactions of trialkoxy-silanes containing terminal donor molecules.[4] This type of surface modification of silica has recently been the subject of much debate.[4a,b,e] It has been shown that the reaction of $(C_2H_5O)_3Si(CH_2)_nPPh_2$ ($n = 3$, 4) with the surface hydroxyl groups on silica leads to significant amounts of side products containing anchored phosphorus oxide species, as well as the oligomerization of trialkoxysilanes in solution.[4a,b] Surface immobilized P^V groups that do not bind tightly to the transition metals contribute to leaching of metals from the surface. We have recently developed a new synthetic methodology[5,6] based on simple acid−base hydrolysis that utilizes commercially available reagents to construct thin films containing amine and phosphine donor ligands on the

(1) (a) Iwasawa, Y.; Gates, B. C. *Chemtech* 1989, 3, 173−181 and references therein. (b) Hartley, F. R. *Supported Metal Complexes, A New Generation of Catalysts*; D. Reidel Publishing: Dordrecht, Netherlands, 1985. (c) *Surface Organometallic Chemistry: Molecular Approaches to Surface Catalysis*; Basset, J. M., Gates, B. C., Candy, J.-P., Choplin, A., Leconte, M., Quignard, F., Santini, C., Eds.; Kluwer: Dordrecht, Netherlands, 1988.
(2) (a) Iwasawa, Y. *Tailored Metal Catalysts*; D. Reidel Publishing: Dordrecht, Netherlands, 1986. (b) Jacobs, P. A.; Bein, T.; De Vos, D. E.; Subba Rao, Y. V. *J. Chem. Soc., Chem. Commun.* 1997, 355−356.
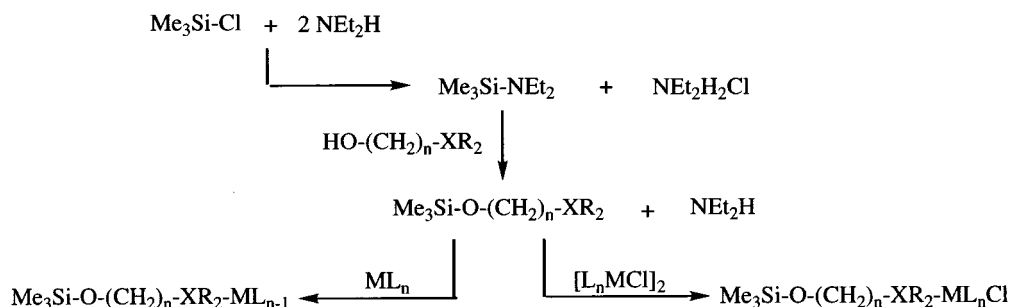(3) Elmer, T. H. In *Silylated Surfaces*; Leyden, D. E., Collins, W. T., Eds.; Gordon and Breach Science Publishers: New York, 1978; p 1.

(4) (a) Blumel, J. *J. Am. Chem. Soc.* 1995, 117, 2112−2113. (b) Blumel, J. *Inorg. Chem.* 1994, 33, 5050−5056. (c) Capka, M.; Czakoova, M.; Wlodzimierz, U.; Schubert, U. *J. Mol. Catal.* 1992, 74, 335. (d) Deschler, U.; Kleinschmit, P.; Panster, P. *Angew. Chem., Int. Ed. Engl.* 1986, 25, 236−252. (e) Bemi, L.; Clark, H. C.; Davies, J. A.; Fyfe, C. A.; Wasylishen, R. E. *J. Am. Chem. Soc.* 1982, 104, 438−445. (f) Allum, K. G.; Hancock, R. D.; Mckenzie, S.; Pitkethly, R. C. *Catal. Proc. Int. Congr., 5th* 1972, 1, 477−486. (g) Smith, A. K.; Basset, J. M.; Maitlis, P. M. *J. Mol. Catal.* 1977, 2, 223−226.
(5) (a) Petrucci, M. G. L.; Kakkar, A. K. *J. Chem. Soc., Chem. Commun.* 1995, 1507−1508. (b) Petrucci, M. G. L.; Kakkar, A. K. *Adv. Mater.* 1996, 8 (3), 251−253.
(6) Yam, C. M.; Kakkar, A. K. *J. Chem. Soc., Chem. Commun.* 1995, 907−909.

Scheme 1

$$Me_3Si\text{-}Cl \ + \ 2\ NEt_2H$$

$$\downarrow$$

$$Me_3Si\text{-}NEt_2 \ + \ NEt_2H_2Cl$$

$$HO\text{-}(CH_2)_n\text{-}XR_2 \ \downarrow$$

$$Me_3Si\text{-}O\text{-}(CH_2)_n\text{-}XR_2 \ + \ NEt_2H$$

$$Me_3Si\text{-}O\text{-}(CH_2)_n\text{-}XR_2\text{-}ML_{n-1} \xleftarrow{\ ML_n\ } \qquad \xrightarrow{\ [L_nMCl]_2\ } Me_3Si\text{-}O\text{-}(CH_2)_n\text{-}XR_2\text{-}ML_nCl$$

surfaces of silica, glass, quartz, and single-crystal Si and avoids many of the common side reactions of the silane condensation methodology mentioned above. It leads to thin films containing terminal phosphine ligands without any surface-bound phosphine oxide species. The anchored donor ligands are subsequently used to carry out ligand-displacement or bridge-splitting reactions to afford covalently surface-bound transition-metal complexes. The flat surfaces of glass, quartz, and single-crystal Si allow for the build up of robust thin films of oriented organometallic moieties. Increasing the number of available metallic sites oriented in a specific direction may significantly enhance catalytic activity and selectivity.[7] In addition, flat surfaces offer opportunities to elucidate the molecular structure of the anchored species by probing the environment of the active metal center involved in catalysis. There are a variety of experimental techniques that can be employed to characterize, identify, and estimate the nature of the surface species, leading to new information for the design of future tailor-made catalysts.

Results and Discussion

Solution Chemistry. Aminosilanes, $(CH_3)_3Si−NR_2$ ($R = CH_3$, C_2H_5), which are generally prepared from organosilicon halides and excess NR_2H, react almost quantitatively via acid−base hydrolysis with molecules containing acidic protons, affording the corresponding silylated alcohols with the elimination of amine (Scheme 1).[8] For example, $Me_3Si−NEt_2$ reacts with terminal alcohols such as $HO−(CH_2)_n−XR_2$, $HO−(C_6H_4)−XR_2$, and $HO−CH(CH_3)−(CH_2)_3−XR_2$ ($X = N$, P) at ambient temperature to yield $Me_3Si−O−C_6H_4−N(C_2H_5)_2$ (**1**), $Me_3Si−O−(CH_2)_3−N(C_2H_5)_2$ (**2**), $Me_3Si−O−CH(CH_3)−(CH_2)_3−N(C_2H_5)_2$ (**3**), $Me_3Si−O−(CH_2)_n−PR_2$ ($n = 4$, R $= C_2H_5$, **4**; $n = 3$, R $= C_6H_5$, **5**), and $Me_3Si−O−C_6H_4−P(C_6H_5)_2$ (**6**) in almost quantitative yields. These tertiary phosphine and amine donor ligands react with organometallic complexes via ligand-displacement or bridge-splitting processes. For example, a phosphine ligand on $Ni(CO)_2(PPh_3)_2$ can be exchanged with $Me_3Si−O−(CH_2)_n−XR_2$ or $Me_3Si−NEt_2$ to give $Me_3Si−O−(CH_2)_3−PPh_2Ni(CO)_2PPh_3$ (**7**), $Me_3Si−O−(CH_2)_4−PEt_2Ni(CO)_2PPh_3$ (**8**), $Me_3SiNEt_2Ni(CO)_2PPh_3$ (**9**), $Me_3Si−O−(CH_2)_3−NEt_2Ni(CO)_2PPh_3$ (**10**), and $Me_3Si−O−CH(CH_3)−(CH_2)_3−NEt_2Ni(CO)_2PPh_3$ (**11**). The displacement or bridge-splitting reactions of the above ligands with $RhCl(CO)(PPh_3)_2$, $RhCl(PPh_3)_3$, or $[RhCl(CO)_2]_2$

similarly gave $Me_3Si−O−(CH_2)_3−PPh_2RhCl(CO)PPh_3$ (**12**), $Me_3Si−O−(CH_2)_3−PPh_2RhCl(CO)_2$ (**13**), $Me_3SiNEt_2RhCl(PPh_3)_2$ (**14**), $Me_3Si−O−(CH_2)_3−NEt_2RhCl(CO)PPh_3$ (**15**), $Me_3Si−O−CH(CH_3)−(CH_2)_3−NEt_2RhCl(CO)PPh_3$ (**16**), and $Me_3Si−O−C_6H_4−NEt_2RhCl(CO)PPh_3$ (**17**). The complexes $Me_3Si−O−(CH_2)_3−PPh_2Pd(PPh_3)_3$ (**18**) and $Me_3Si−O−(CH_2)_3−PPh_2RuCl_2(CO)_2PPh_3$ (**19**) were accordingly prepared by reacting the appropriate ligand with $Pd(PPh_3)_4$ or $RuCl_2(CO)_2(PPh_3)_2$, respectively.

The solution $^{31}P\{^1H\}$ NMR and the FT-IR data for the above-mentioned Ni, Rh, Pd, and Ru complexes are shown in Table 1. The $^{31}P\{^1H\}$ NMR spectra are similar to those for their starting complexes with some exceptions. The compound $Me_3Si−O−(CH_2)_3−NEt_2Ni(CO)_2PPh_3$ produced a singlet at 26.7 ppm in its $^{31}P\{^1H\}$ NMR spectrum which is similar to that for $Me_3SiNEt_2Ni(CO)_2PPh_3$ (singlet at 27.3 ppm) and $Me_3Si−O−CH(CH_3)(CH_2)_3−NEt_2Ni(CO)_2PPh_3$ (27.3 ppm, s) and, intriguingly, is shifted upfield compared to the bis(phosphine) complex $Ni(CO)_2(PPh_3)_2$ (35.2 ppm). Such a shift in the $^{31}P\{^1H\}$ NMR spectrum is generally observed upon replacing a triarylphosphine with a more electron-donating trialkylphosphine at the metal center. For example, replacement of one of the PPh_3 ligands on $Ni(CO)_2(PPh_3)_2$ with a trialkylphosphine, $Me_3Si−O−(CH_2)_4−PEt_2Ni(CO)_2PPh_3$, leads to an upfield shift (26.3 ppm). A similar shift is also observed upon comparing $Me_3Si−O−(CH_2)_3−PPh_2Pd(PPh_3)_3$ (13.72 ppm) with the starting complex $Pd(PPh_3)_4$ (19.6 ppm).

The compound $Me_3SiNEt_2RhCl(PPh_3)_2$, which was prepared by the reaction of $RhCl(PPh_3)_3$ with Me_3SiNEt_2, showed only a doublet at 54.5 ppm ($J_{Rh−P} = 195$ Hz) in its $^{31}P\{^1H\}$ NMR spectrum, suggesting a square-planar geometry for this complex with two equivalent phosphines.

A comparison of the FT-IR spectra of the Ni(0) complexes also showed some intriguing results. The bisphosphine complexes $Me_3Si−O−(CH_2)_4−PEt_2Ni(CO)_2PPh_3$ and $Me_3Si−O−(CH_2)_3−PPh_2Ni(CO)_2PPh_3$ exhibit two ν_{CO} stretching frequencies similar to those for $Ni(CO)_2(PPh_3)_2$ (Table 1). However, it is interesting to note that for the complexes in which one of the phosphines is replaced with an amine ligand, $Me_3SiNEt_2Ni(CO)_2PPh_3$, $Me_3Si−O−(CH_2)_3−NEt_2Ni(CO)_2PPh_3$, and $Me_3Si−O−CH(CH_3)(CH_2)_3−NEt_2Ni(CO)_2PPh_3$, the ν_{CO} stretching frequencies move to lower wavenumbers. This trend is not observed for the Rh(I) complexes.

The $^{31}P\{^1H\}$ NMR and FT-IR spectra for the above solution models are valuable in evaluating and comparing the structures of the surface-immobilized transition-

(7) Tollner, K.; Popovitz-Biro, R.; Lahav, M.; Milstein, D. *Science* **1997**, *278*, 2100.

(8) Fessenden, R.; Fessenden, J. S. *Chem. Rev.* **1961**, *61*, 361.

Table 1. High-Resolution Solution $^{31}P\{^1H\}$ NMR and FT-IR Data for Organometallic Complexes Containing Nitrogen and Phosphorus Donor Ligands

complex	$^{31}P\{^1H\}$, C_6D_6 δ (ppm)	FT-IR, ν_{CO} (cm^{-1}) Nujol
$(CH_3)_3Si-O-(CH_2)_4PEt_2$ (**4**)	−21.7	
$(CH_3)_3Si-O-(CH_2)_3PPh_2$ (**5**)	−14.1	
$(CH_3)_3Si-O-C_6H_4PPh_2$ (**6**)	25.6	
$Ni(CO)_2(PPh_3)_2$	35.2	1998, 1935
$(CH_3)_3Si-O-(CH_2)_3PPh_2Ni(CO)_2PPh_3$ (**7**)	34.0 (d), 25.1 (d)	1999, 1938
$(CH_3)_3Si-O-(CH_2)_4PEt_2Ni(CO)_2PPh_3$ (**8**)	27.1 (d), 26.3 (d)	1996, 1934
$(CH_3)_3SiNEt_2Ni(CO)_2PPh_3$ (**9**)	27.3	1981, 1934
$(CH_3)_3Si-O-(CH_2)_3NEt_2Ni(CO)_2PPh_3$ (**10**)	26.7	1982, 1936
$(CH_3)_3Si-O-CH(CH_3)(CH_2)_3NEt_2Ni(CO)_2PPh_3$ (**11**)	26.9	1975, 1916
$RhCl(PPh_3)_3$	33.3 (d), 54.6 (dd)	
$[RhCl(CO)_2]_2$		2105, 2085, 2031
$RhCl(CO)(PPh_3)_2$	31.9 (d)	1960
$(CH_3)_3Si-O-(CH_2)_3PPh_2RhCl(CO)PPh_3$ (**12**)	23.7 (d), 24.4 (d)	1964
$(CH_3)_3Si-O-(CH_2)_3PPh_2RhCl(CO)_2$ (**13**)	27.2 (d)	2080, 2010
$(CH_3)_3SiNEt_2RhCl(PPh_3)_2$ (**14**)	54.5 (d)	
$(CH_3)_3Si-O-(CH_2)_3NEt_2RhCl(CO)PPh_3$ (**15**)	46.7 (d)	1968
$(CH_3)_3Si-O-CH(CH_3)(CH_2)_3NEt_2RhCl(CO)PPh_3$ (**16**)	46.4 (d)	1961
$(CH_3)_3Si-O-C_6H_4NEt_2RhCl(CO)PPh_3$ (**17**)	47.9 (d)	1964
$Pd(PPh_3)_4$	19.6	
$(CH_3)_3Si-O-(CH_2)_3PPh_2Pd(PPh_3)_3$ (**18**)	13.72 (br)	
$RuCl_2(CO)_2(PPh_3)_2$	18.5	2054, 1996
$(CH_3)_3Si-O-(CH_2)_3PPh_2RuCl_2(CO)_2PPh_3$ (**19**)	20.5, 19.2	2062, 1982

Scheme 2

M= Rh, Ni, Pd, Ru
L= CO, PR$_3$
X= N, P
R= Et, Ph
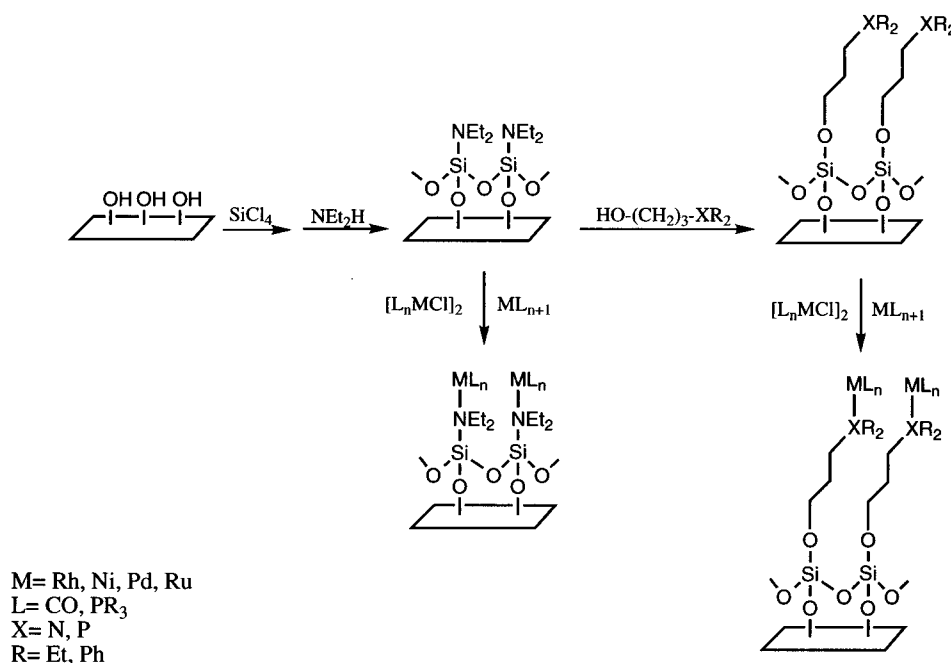
metal complexes. Solution models also provide essential information concerning the reaction conditions for surface deposition. The above-described acid−base hydrolytic chemistry of aminosilanes with species containing terminal acidic protons, if easily transferred to inorganic oxide surfaces, can provide a simple and efficient method for anchoring phosphine and amine donor ligands and subsequently building covalently immobilized organometallic thin films.

Surface Chemistry and Characterization. It is well-known that the surfaces of silica, glass, quartz, and single-crystal silicon consist of Si−OH groups with a packing density of approximately 4.70 OH/100 Å^2.[9a] Before any deposition process, the inorganic oxide substrates used in this study were cleaned[9b,c] by (i) soaking in soap solution and sonicating for 30 min; (ii) treating with piranha solution (70% H$_2$SO$_4$, 30% H$_2$O$_2$)

[**Caution**: The piranha solution is highly corrosive and explosive. Care should be taken while using this mixture]; (iii) rinsing with deionized water; and, finally, (iv) drying over a stream of nitrogen. Thin films containing terminal donor ligands were deposited by treating the substrates with toluene solutions of (i) SiCl$_4$, (ii) dry NEt$_2$H, and (iii) the appropriate donor ligands (Scheme 2). These thin films containing terminal phosphine and amine ligands were then utilized to covalently anchor transition-metal complexes by displacement[4f] or bridge-splitting[10−13] reactions similar to the solution chemistry described above.

(9) (a) Zhuravlev, L. T. *Colloids and Surf.* **1993**, 74 (1), 71. (b) Lloyd, T. B.; Li, J.; Fowkes, F. M.; Brand, J. R.; Dizikes, L. J. *J. Coat. Technol.* **1992**, *64*, (813), 91−99. (b) Pintchovski, F.; Pricew, J. B.; Tobin, P. J.; Peavey, J.; Kobold, K. *J. Electrochem. Soc.* **1979**, 1428. (c) Wasserman, S. R.; Yu-Tai, T.; Whitesides, G. M. *Langmuir* **1990**, *6*, 1074.

(10) Ugo, R.; Bonati, F.; Fiore, M. *Inorg. Chim. Acta* **1968**, *2*, 463.

Some of the commonly used techniques for the characterization and estimation of the structure of the newly prepared thin films containing surface-immobilized species include contact angle goniometry, X-ray photoelectron, solid-state NMR, and FT-IR (transmission and attenuated total reflection modes) spectroscopies. The results from a combination of these techniques provide a useful estimation of the surface composition as well as the environment of the surface-bound metal center involved in catalysis. A summary of the techniques employed in this study is given below.

Contact Angle Goniometry. To gain some insight into the structure and packing of the surface-bound species, thin films containing terminal amine and phosphine donor ligands on flat surfaces were characterized by surface-wettability measurements. Contact angle goniometry measures the angle that the drop of a liquid makes on a flat substrate and is dependent on the relative hydrophobicity or hydrophilicity of the thin film surface and the liquid.[14a] For example, a clean and unfunctionalized glass surface produces a contact angle of ~18° with water. When a nonpolar liquid such as hexadecane is deposited onto a hydrophilic surface such as an unfunctionalized glass slide, an increase in the forces of repulsion at the solid−liquid interface results in a higher contact angle (~85°). Conversely, when hexadecane is deposited onto an organic monolayer, an increase in the forces of attraction results in the lowering of the contact angle. Thin films containing tertiary phosphines (phenyl-, propyl-, and butylphosphines) exhibited contact angles of around 7° with hexadecane and an average of 95° with a polar probe liquid such as deionized H_2O. These values are consistent with, for example, anchored structures exposing phenyl groups or short chain alkanes to the surface[14b−d] and suggest that these surface-bound phosphines are densely packed. We were unable to examine the contact angle for the surface-anchored [Si]−NEt_2 moieties, since the Si−N bond can be easily hydrolyzed. The thin films containing long alkane chain nitrogen-donor ligands (phenyl-, propyl-, and pentylamines) produced contact angles ranging between 68° and 74° with water, which are lower than for the phosphine-terminated surfaces. Such lower contact angles have also been observed for surface-bound 4′-(4-methylphenyl)-2,2′:6′,2″-terpyridine ligand[14e] and may, probably, be due to the more polar nature of the nitrogen atom of the terminal amine ligands.

UV−Vis Absorption Spectroscopy. UV−Vis absorption spectroscopy has been used in the past for the evaluation of the packing density in newly developed thin film structures.[15a,b] The UV−vis absorption spectrum of $Ni(CO)_2(PPh_3)_2$ in solution shows a peak at 236 nm, and a similar spectrum for the anchored Ni(0) complex [Si]−O−$(CH_2)_3$−$PPh_2Ni(CO)_2(PPh_3)$ gives the absorption maxima at 208 nm with a blue shift of ~28 nm. A similar blue shift (~50 nm) in the UV−vis absorption spectra has also been observed upon immobilizing a cobalt(II) acetate complex.[15c] An estimation of the surface coverage in a thin film of [Si]−O−$(CH_2)_2$−$PPh_2Ni(CO)_2(PPh_3)$ on quartz by UV−vis absorption spectroscopy gives a surface packing density of 3×10^{-9} mol/cm^2, which is comparable to coverages reported previously for covalently anchored monolayers of metal complexes,[15a−c] and suggests a densely packed thin film.

X-ray Photoelectron Spectroscopy (XPS). XPS is known to be a very good technique for the determination of the surface composition of the anchored species, and it can provide useful information about the elements present on the surface. In addition, changing the substituents on the metal center results in an increase or decrease in the binding energies of the metal and the elements of the donor ligands attached to it. We applied this technique for the analytical evaluation of various organometallic complexes immobilized on glass slides (Table 2b). For a comparative study, XPS spectra of the model complexes were also collected and the results are presented in Table 2a.

We first attempted an evaluation of the efficiency of the reactions of $SiCl_4$ with surface hydroxyl groups, followed by the reaction with NEt_2H, and finally with the appropriate phosphine or amine donor molecules (steps 1−3, Scheme 2). No residual chlorine or amine was found from a detailed XPS analysis of these thin films, which suggests high conversion of the surface-bound chlorine to amine and, finally, phosphine/amine donor moieties.

There is a slight increase in the binding energies of the elements in the thin films as compared to their solid-state analogues (Table 2). For example, the P 2s line positions for the thin films range between 197.9 and 204.6 eV. These binding energies are slightly shifted from the model complexes (188−197 eV) as well as from the known value of 191 eV for free PPh_3.[16] An increase in the binding energies is also apparent for the Si 2p, O 1s, and C 1s peaks of the surface-immobilized metal complexes. This increase in the binding energies of the respective elements in the thin films may be due to charging effects. Since electrons are leaving the sample by photoemission, an electrical equilibrium can only be established if electrons can readily flow from ground to neutralize the residual positive charge. For insulators such as glass, the conductivity may not be sufficient to prevent positive charge build up, thereby resulting in an increase in the binding energies. The Si 2p binding energies for the thin films are greatly affected by charging, resulting in the largest difference in binding energies from the model complexes.

One should be cautious in interpreting XPS spectra, however, besides charging, there are other effects

(11) Heiber, W.; Heusinger, H.; Vohler, J. *Chem. Ber.* **1957**, *90*, 2425.

(12) Lawson, D. N.; Wilkinson, G. *J. Chem. Soc.* **1965**, 1900.

(13) Rollman, L. D. *Inorg. Chim. Acta* **1972**, *6*, 137.

(14) (a) Ulman, A. *Introduction to Ultrathin Films. From Langmuir Blodgett to Self-Assembly*; Academic: New York, 1991. (b) Dhirani, A.-A.; Zehner, R. W.; Hsung, R. P.; Guyot-Sionnest, P.; Sita, L. R. *J. Am. Chem. Soc.* **1996**, *118*, 3319. (c) Sabatini, E.; Cohen- Boulakio, J.; Bruening, M.; Rubinstein, I. *Langmuir* **1993**, *9*, 2974. (d) Fox, H. W.; Hare, E. F.; Zisman, W. A. *J. Colloid Sci.* **1953**, *8*, 194. (e) Schmehl, R. H.; Liang, Y. *J. Chem. Soc., Chem. Commun.* **1995**, 1007.

(15) (a) Sullivan, P. B.; Morris, K.; Paulson, S. *J. Chem. Soc., Chem. Commun.* **1992**, 1615. (b) Li, D.; Swanson, B. I.; Robinson, J. M.; Hoffbauer, M. A. *J. Am. Chem. Soc.* **1993**, *155*, 6975. (c) Butterworth, J. H.; Clark, J. H.; Walton, P. H.; Barlow, S. J. *J. Chem. Soc., Chem. Commun.* **1996**, 1859. (d) Arkles, B. Silane Coupling Agent Chemistry. In *Silane Compounds: Register and Review*; Arkles, B., Anderson, P., Larsen, G. L., Petrach Systems, Bristol, PA, 1987. (e) The surface coverage (3×10^{-9} mol/cm^2) was calculated using UV−vis absorption spectroscopy: [Si]−O−$(CH_2)_3PPh_2Ni(CO)_2PPh_3$, $\lambda_{max} = 208$ nm, $A = 0.20$; $Ni(CO)_2(PPh_3)_2$, λ_{max} 236 nm), $A = 2.55$.

(16) Tolman, C. A.; Riggs, W. M.; Linn, W. J.; King, C. M.; Wendt, R. C. *Inorg. Chem.* **1973**, *12* (12), 2770.

Table 2. Binding Energies (eV)

a. Organometallic Complexes

complex	Si2p3/2	FWHM	O1s1/2	FWHM	C1s1/2	FWHM	P2s1/2	FWHM	N1s1/2	FWHM	Cl2s1/2	FWHM	Ni2p3/2	FWHM
Me3SiO(CH2)4PEt2Ni(CO)2PPh3 (8)	98.0	2.00	531.0	5.00	280.0	3.00	188.0	3.00					852.0	4.00
Me3SiO(CH2)3NEt2Ni(CO)2PPh3 (10)	97.0	3.00	528.0	3.00	280.0	3.00	192.0	3.00	394.0	3.00			850.0	3.00
Me3SiOCH(CH3)(CH2)3NEt2Ni(CO)2PPh3 (11)	97.0	2.50	527.0	6.00	279.0	2.00	192.0	6.00	394.0	2.50			849.0	2.50

complex	Si2p3/2	FWHM	O1s1/2	FWHM	C1s1/2	FWHM	P2s1/2	FWHM	N1s1/2	FWHM	Cl2s1/2	FWHM	Rh3d5/2	FWHM
Me3SiO(CH2)3PPh2RhCl(CO)PPh3 (12)	97.0	3.00	528.0	4.00	281.0	4.00	192.0	3.00			269.0	4.00	309.0	2.50
Me3SiO(CH2)3PPh2Rh(CO)2Cl (13)	97.0	3.00	527.0	3.00	280.0	3.00	193.0	3.00			264.0	3.00	308.0	2.50
Me3Si—NEt2RhCl(PPh3)3 (14)	97.0	3.00	528.0	3.00	280.0	3.00	193.0	3.00	395.0	2.00	264.0	3.00	309.0	2.50
Me3SiOCH(CH3) (CH2)3NEt2RhCl (CO)PPh3 (16)	97.0	3.00	528.0	3.00	280.0	3.50	193.0	3.50	395.0	3.00	267.0	3.50	312.0	2.00

complex	Si2p3/2	FWHM	O1s1/2	FWHM	C1s1/2	FWHM	P2s1/2	FWHM	N1s1/2	FWHM	Cl2s1/2	FWHM	Pd3d5/2	FWHM
Me3SiO(CH2)3PPh2Pd(PPh3)3 (18)	98.0	3.00	528.0	3.00	528.0	4.00	280.0	2.50	188.0	1.00			337.0	3.00

complex	Si2p3/2	FWHM	O1s1/2	FWHM	C1s1/2	FWHM	P2s1/2	FWHM	N1s1/2	FWHM	Cl2s1/2	FWHM	Ru3p1/2	FWHM
Me3SiO(CH2)3PPh2RuCl2(CO)2PPh3 (19)	98.0	6.00	529.0	7.00	280.0	7.00	197.0	6.00			271.0	7.00	482.0	7.00

b. Surface-Bound Organometallic Complexes

thin film	Si2p1/2	FWHM	O1s1/2	FWHM	C1s1/2	FWHM	P2s1/2	FWHM	N1s1/2	FWHM	Cl2s1/2	FWHM	Ni2p3/2	FWHM
[Si]O(CH2)3PPh2Ni(CO)2PPh3 (26)	102.6	8.00	532.0	9.00	284.9	9.00	199.0	8.00					859.0	12.00
[Si]O(CH2)4PEt2Ni(CO)2PPh3 (27)	102.5	8.00	530.2	9.00	287.0	9.00	198.2	9.00					858.0	12.00
[Si]—NEt2Ni(CO)2PPh3 (28)	105.9	9.00	531.0	9.00	286.2	9.00	199.5	8.00	401.5	8.00			858.0	13.00
[Si]O(CH2)3NEt2Ni(CO)2PPh3 (29)	109.3	8.00	531.6	10.00	288.2	9.00	203.5	9.00	400.7	9.00			856.0	12.00
[Si]OCH(CH3)(CH2)3NEt2Ni(CO)2PPh3 (30)	106.6	8.00	530.9	9.00	286.9	9.00	200.6	9.00	400.2	8.00			856.0	11.00

thin film	Si2p1/2	FWHM	O1s1/2	FWHM	C1s1/2	FWHM	P2s1/2	FWHM	N1s1/2	FWHM	Cl2s1/2	FWHM	Rh3d5/2	FWHM
[Si]O(CH2)3PPh2Rh(CO)2Cl (31)	103.4	9.00	531.7	9.00	285.1	8.00	198.2	9.00			269.6	8.00	310.4	11.00
[Si]O(CH2)3PPh2RhCl(CO)PPh3 (32)	103.7	9.00	530.8	9.00	284.9	9.00	199.8	8.00			269.2	7.00	307.7	9.00
[Si]—NEt2RhCl(PPh3)3 (33)	109.5	9.00	533.0	9.00	289.7	9.00	204.6	8.00	401.8	9.00	270.8	8.00	315.2	10.00
[Si]O(CH2)3NEt2RhCl(CO)PPh3 (34)	103.0	9.00	531.0	9.00	285.7	8.00	197.9	9.00	399.5	8.00	268.7	7.00	310.8	10.00
[Si]OCH(CH3)(CH2)3NEt2RhCl(CO)PPh3 (35)	105.5	9.00	531.3	9.00	286.6	8.00	200.3	8.00	400.1	8.00	270.9	8.00	311.8	10.00
[Si]OC6H4NEt2RhCl(CO)PPh3 (36)	105. 3	9.00	531.0	9.00	286.4	8.00	200.3	8.00	398.9	8.00	269.7	8.00	311.6	10.00

thin film	Si2p1/2	FWHM	O1s1/2	FWHM	C1s1/2	FWHM	P2s1/2	FWHM	N1s1/2	FWHM	Cl2s1/2	FWHM	Pd3d1/2	FWHM
[Si]O(CH2)3PPh2Pd(PPh3)3 (37)	104.2	4.00	534.3	4.00	286.0	2.00	195.2	4.00					338.2	2.00

thin film	Si2p1/2	FWHM	O1s1/2	FWHM	C1s1/2	FWHM	P2s1/2	FWHM	N1s1/2	FWHM	Cl2s1/2	FWHM	Ru3p1/2	FWHM
[Si]O(CH2)3PPh2RuCl2(CO)2PPh3 (38)	105.3	10.00	531.0	9.00	287.2	9.00	201.1	10.00			271.0	8.00	489.0	8.00

Table 3. CP/MAS $^{31}P\{^1H\}$ NMR and FT-IR Data for Anchored Complexes Containing Phosphorus and Nitrogen Donor Ligands

thin film ([Si] = ground glass silica)	$^{31}P\{^1H\}$ CP/MAS δ (ppm)	FT-IR, KBr ν_{CO} (cm^{-1})
[Si]−O−C$_6$H$_4$PPh$_2$ (**20**)	26.7	
[Si]−O−(CH$_2$)$_3$PPh$_2$ (**21**)	−16.01	
[Si]−O−(CH$_2$)$_4$PEt$_2$ (**22**)	−23.2	
[Si]−O−(CH$_2$)$_3$PPh$_2$Ni(CO)$_2$PPh$_3$ (**26**)	29.5 (br)^a	1998, 1934
[Si]−O−(CH$_2$)$_4$PEt$_2$Ni(CO)$_2$PPh$_3$ (**27**)	28.1, 28.8	1996, 1932
[Si]−NEt$_2$Ni(CO)$_2$PPh$_3$ (**28**)	31.2	1980, 1936
[Si]−O−(CH$_2$)$_3$NEt$_2$Ni(CO)$_2$PPh$_3$ (**29**)	28.8	1982, 1935
[Si]−O−CH(CH$_3$)(CH$_2$)$_3$NEt$_2$Ni(CO)$_2$PPh$_3$ (**30**)	28.4	1975, 1911
[Si]−O−(CH$_2$)$_3$PPh$_2$Rh(CO)$_2$Cl (**31**)	23.4	2079, 2001
[Si]−O−(CH$_2$)$_3$PPh$_2$RhCl(CO)PPh$_3$ (**32**)	28.2, 33.2	1964
[Si]−NEt$_2$RhCl(PPh$_3$)$_2$ (**33**)	51.1, 58.3	
[Si]−O−(CH$_2$)$_3$NEt$_2$RhCl(CO)PPh$_3$ (**34**)	47.5	1958
[Si]−O−CH(CH$_3$)(CH$_2$)$_3$NEt$_2$RhCl(CO)PPh$_3$ (**35**)	48.6	1954
[Si]−O−C$_6$H$_4$NEt$_2$RhCl(CO)PPh$_3$ (**36**)	47.5	1956
[Si]−O−(CH$_2$)$_3$PPh$_2$Pd(PPh$_3$)$_3$ (**37**)	14.6 (br)^a	
[Si]−O−(CH$_2$)$_3$PPh$_2$RuCl$_2$(CO)$_2$PPh$_3$ (**38**)	17.5 (br)^a	2054, 1996

^{a} br = broad.

related to coordination of the ligands to the metal and the presence of electron-withdrawing elements on the metal center that might cause shifts in binding energies. We observe that as poor donor ligands such as amines replace phosphines at the metal center, there is an increase in the binding energies of P 2s (Table 2). For the surface-anchored complexes containing only the phosphine donor ligands, the Rh binding energies ranged between 307.7 and 310.3 eV, which are comparable to the binding energies for the solution model complexes (308−309 eV) as well as the known value of 309 eV for RhCl(CO)(PPh$_3$)$_2$.[17] However, a similar increase in the binding energies as that observed for P 2s energies was also evident for the Rh 3d$_{5/2}$ binding energies of complexes containing amine donor ligands. The Cl 1s energies were found to be in the range of 268.7−271.0 eV for the surface-bound species. The higher value of 271.0 eV for [Si]−O−(CH$_2$)$_3$PPh$_2$-RuCl$_2$(CO)$_2$PPh$_3$ may also be due to the presence of two chloride ligands on the metal center. This is also seen for the model complex, RuCl$_2$(CO)$_2$PPh$_3$[PPh$_2$(CH$_2$)$_3$-OSiMe$_3$] (**16**).

Solid-State $^{31}P\{^1H\}$ NMR. The application of cross-polarization[18] and magic-angle spinning[19] techniques in the solid-state $^{31}P\{^1H\}$ NMR spectroscopy is extremely valuable when studying surface-immobilized transition metal complexes containing phosphorus(III) donors.[4a,b,e] For instance, thin films containing terminal phosphines on ground glass [Si]−O−(CH$_2$)$_3$PPh$_2$ and [Si]−O−(CH$_2$)$_4$-PEt$_2$ exhibit single resonances at δ −16.01 and −23.2 ppm, respectively, in their cross-polarized $^{31}P\{^1H\}$ NMR spectra (Table 3). These resonances are comparable with the high-resolution solution $^{31}P\{^1H\}$ NMR spectra of Me$_3$Si−O−(CH$_2$)$_3$PPh$_2$ (δ −14.05) and Me$_3$Si−O−

(CH$_2$)$_4$PEt$_2$ (δ −21.7) and the $^{31}P\{^1H\}$ CP/MAS NMR of the surface-immobilized P(III) species e.g., [Si]−O−(CH$_2$)$_3$PPh$_2$ (−16.3 ppm), prepared by condensation of (EtO)$_3$Si(CH$_2$)$_3$PPh$_2$ on silica.[4b] As mentioned earlier, the preparation of thin films by the condensation of (EtO)$_3$Si−(CH$_2$)$_n$PPh$_2$ (n = 2, 3) on silica results in the formation of two chemically distinct phosphorus moieties on the surface of the support, specifically the desired phosphine ligand and anchored pentacoordinate phosphine oxide Ph$_2$P(−O−[SiO$_2$]$_2$)$_2$(CH$_2$)$_3$Si−O−[SiO$_2$] (25.9 ppm).[4b] A major concern in the study of immobilized catalysts is their tendency to leach from the support, and it has been suggested that the formation of P(V) species may be a contributing factor for the leaching process[4a,b] The presence of only the surface-bound phosphorus(III) ligand in the acid−base hydrolytic method described here suggests that the new surface functionalization technique is an efficient procedure in preparing phosphine-oxide-free supports under mild reaction conditions.

The solid-state $^{31}P\{^1H\}$ NMR spectra of the covalently anchored Ni(0) organometallic thin films [Si]−O−(CH$_2$)$_3$−PPh$_2$Ni(CO)$_2$PPh$_3$, [Si]−O−(CH$_2$)$_4$−PEt$_2$Ni(CO)$_2$PPh$_3$, and [Si]−NEt$_2$Ni(CO)$_2$PPh$_3$ with isotropic chemical shifts of δ 29.5 (br), 28.8 and 28.1, and 32.2 ppm, respectively, are comparable to their solution models Ni-(CO)$_2$(PPh$_3$)$_2$ (35.2 ppm), (CH$_3$)$_3$Si−O−(CH$_2$)$_3$−PPh$_2$Ni-(CO)$_2$PPh$_3$ (36.0, 26.4 ppm), (CH$_3$)$_3$Si−O−(CH$_2$)$_4$−PEt$_2$-Ni(CO)$_2$PPh$_3$ (27.1, 26.3 ppm), and (CH$_3$)$_3$Si−NEt$_2$Ni-(CO)$_2$PPh$_3$ (27.2 ppm) and to the $^{31}P\{^1H\}$ CP/MAS NMR spectra of (CH$_3$)$_3$Si−O−(CH$_2$)$_3$NEt$_2$Ni(CO)$_2$PPh$_3$ (**28.3** ppm) and (CH$_3$)$_3$Si−O−CH(CH$_3$)(CH$_2$)$_3$NEt$_2$Ni(CO)$_2$PPh$_3$ (31.1 ppm). Similar observations can be made for the Rh(I), Pd(II), and Ru(II) complexes (Tables 1, 3, and 4). Following surface reactions with the organometallic complexes, the isotropic chemical shifts belonging to the bound ligands were no longer observed. The latter implies high efficiency of the displacement and bridge-splitting reactions.

The isotropic chemical shifts and the coupling constant values for the surface-bound species can be compared with those obtained from solution measurements and can assist in assigning the geometry of the surface-bound species. For example, the CP/MAS ^{31}P-$\{^1H\}$ NMR spectrum of [Si]−O−(CH$_2$)$_3$−PPh$_2$RhCl(CO)-PPh$_3$ results in an ABX spin system (where A and B are the magnetically nonequivalent, mutually trans phosphorus nuclei and X is Rh), exhibiting coupling of phosphorus to rhodium and between inequivalent phosphines. The magnitude of J_{Rh-P} coupling of 132 Hz is comparable to that in solution for the RhCl(CO)(PPh$_3$)$_2$ complex (J_{Rh-P} = 127 Hz) and for the (CH$_3$)$_3$Si−O−(CH$_2$)$_3$PPh$_2$RhCl(CO)PPh$_3$ complex in the solid state (J_{Rh-P} = 125 Hz) and is indicative of the silica-bound trans isomer. In contrast, the chelate type phosphine complex would result in a very different J_{Rh-P} coupling, typically 158 Hz (*cis*-[RhCl(CO){PPh$_2$(CH$_2$)$_2$PPh$_2$}]).[20]

The chemical shift anisotropies ($\Delta\sigma$) similarly provide important structural information for the surface-bound complexes of Ni(0), Rh(I), and Ru(II). Chemical shift anisotropies are sensitive enough to differentiate between the chemical environments and bonding arrangements of the phosphorus(III) nuclei.[4b,e,18,19] The chemi-

(17) Grimblot, J.; Bonnelle, J. P.; Montreux, A.; Petit, F. *Inorg. Chim. Acta* **1979**, *34*, 29.

(18) Schaefer, J.; Stejskal, E. O. *J. Am. Chem. Soc.* **1976**, *98*, 1031.

(19) (a) Pines, A.; Gibby, M. G.; Waugh, J. S. *J. Chem. Phys.* **1972**, *56*, 1776; **1973**, *59*, 569. (b) Harris, R. K.; Merwin, L. H.; Hagele, G. *J. Chem. Soc., Faraday Trans 1* **1989**, *85* (6), 1409−1434. (c) Herzfeld, J.; Berger, A. E. *J. Chem. Phys.* **1980**, *73*, 6021. (d) Hargé, J. C.; Abdallaoui, H. E.; Rubini, P. *Magn. Reson. Chem.* **1993**, *31*, 752−757.

(20) Sanger, A. R. *J. Chem. Soc., Chem. Commun.* **1995**, 907−909.

Table 4. $^{31}P\{^1H\}$ NMR Chemical Shift Tensors for Complexes Containing Phosphorus and Nitrogen Donor Ligands Calculated from CP-MAS and Spinning Sideband Analysis[a]

complex	$^{31}P\{^1H\}$ CP/MAS δ (ppm)	δ_{11} (ppm)	δ_{22} (ppm)	δ_{33} (ppm)	$\Delta\sigma^b$ (ppm)
a. Nonanchored Complexes					
$(CH_3)_3Si-O-(CH_2)_4PEt_2Ni(CO)_2PPh_3$ (**8**)	31.1, 25.8	67.8	54.1	−27.35	88.3
$(CH_3)_3Si-O-(CH_2)_3NEt_2Ni(CO)_2PPh_3$ (**10**)	28.3	66.4	53.9	−35.5	95.7
$(CH_3)_3Si-O-CH(CH_3)(CH_2)_3NEt_2Ni(CO)_2PPh_3$ (**11**)	31.1	78.3	45.2	−30.7	92.5
$(CH_3)_3Si-O-(CH_2)_3PPh_2RhCl(CO)PPh_3$ (**12**)	27.5, 23.4	62.3	43.8	−29.8	82.9
$(CH_3)_3Si-O-(CH_2)_3PPh_2Rh(CO)_2Cl$ (**13**)	24.9	78.0	33.5	−37.8	93.6
$(CH_3)_3Si-NEt_2RhCl(PPh_3)_2$ (**14**)	56.2	112.5	66.8	−10.6	100.3
$(CH_3)_3Si-O-CH(CH_3)(CH_2)_3NEt_2RhCl(CO)PPh_3$ (**16**)	43.0	72.8	30.6	−30.6	82.3
$(CH_3)_3Si-O-(CH_2)_3PPh_2RuCl_2(CO)_2PPh_3$ (**19**)	19.8, 17.0	70.2	19.4	−35.8	80.6
b. Anchored Complexes					
$[Si]-O-C_6H_4PPh_2{}^c$ (**20**)	26.7	62.3	28.4	−10.2	55.6
$[Si]-O-(CH_2)_3PPh_2{}^c$ (**21**)	−16.6	13.8	−21.3	−42.2	49.7
$[Si]-O-(CH_2)_4PEt_2Ni(CO)_2PPh_3{}^c$ (**27**)	28.1, 28.8	75.8	41.2	−30.8	89.3
$[Si]-O-(CH_2)_3NEt_2Ni(CO)_2PPh_3{}^c$ (**29**)	28.8	83.4	44.5	−41.6	105.6
$[Si]-O-CH(CH_3)(CH_2)_3NEt_2Ni(CO)_2PPh_3{}^c$ (**30**)	28.4	72.0	50.4	−37.2	98.4
$[Si]-O-(CH_2)_3PPh_2Rh(CO)_2Cl^c$ (**31**)	23.4	74.8	31.7	−36.8	90.1
$[Si]-O-(CH_2)_3PPh_2RhCl(CO)PPh_3{}^c$ (**32**)	28.2, 31.5	84.4	37.1	−27.1	87.8
$[Si]-NEt_2RhCl(PPh_3)_2{}^c$ (**33**)	51.1, 58.3	104.9	72.4	−13.2	101.9
$[Si]-O-CH(CH_3)(CH_2)_3NEt_2RhCl(CO)PPh_3{}^c$ (**35**)	48.6	87.8	61.7	−5.5	80.3
$[Si]-O-(CH_2)_3PPh_2RuCl_2(CO)_2PPh_3{}^c$ (**38**)	17.5 (br)^d	69.2	22.5	−32.7	78.6

[a] Uncertainties are ±1.5 and ±2.5 ppm for the chemical shift tensors and $\Delta\sigma$, respectively. [b] Anisotropy parameter $\Delta\delta = \delta_{33} - {}^1\!/{}_2(\delta_{11} + \delta_{22})$, where $|\delta_{33} - \delta_{iso}| > |\delta_{11} - \delta_{iso}| > |\delta_{22} - \delta_{iso}|$, $\delta = -\sigma$. [c] [Si] = ground glass silica. [d] br = broad.

cal shift anisotropies (CSAs) in the $^{31}P\{^1H\}$ CP/MAS NMR spectra of tertiary phosphine ligands have been reported to be in the range of 35−50 ppm.[4e] In the present study, CSAs for the immobilized phosphines $[Si]-O-C_6H_4-PPh_2$ (**20**) and $[Si]-O-(CH_2)_3PPh_2$ (**21**) were found to be 56 and 50 ppm, respectively. The phosphorus(V) nuclei generally exhibit greater deshielding in comparison to the phosphorus(III) nuclei and, thus, result in a larger anisotropy (190 ppm for OP-$(C_{14}H_{29})_3$ and 200 ppm for OPPh$_3$).[4e]

The chemical shifts and chemical shift anisotropies of the supported metal complexes are similar to those for the unbound complexes (Table 4), suggesting that the organometallic complexes retain their structures on the surface. The CSAs of the surface-immobilized organometallic species range between 76 and 106 ppm, which indicates that there are no P(V)-anchored species on the surface. Transition-metal complexes bound by phosphorus ligands generally exhibited lower anisotropies than metal complexes covalently bound to amine donor ligands. Since amine ligands are weaker donors than phosphines, they have a much more profound deshielding effect on the anisotropic chemical shift of phosphorus.

FT-IR Spectroscopy. Fourier transform infrared spectroscopy in the transmission and attenuated total reflection (ATR) modes was applied to characterize the structure of bound organometallic moieties containing carbonyl ligands. FT-IR-ATR, in particular, is very useful in characterizing thin film structures.[5b] This sensitive surface technique provides insight into the environment of the active metal center, the ligands present, and the packing arrangement onto the flat silicon substrates. The organometallic thin films of $\{Si\}-O-(CH_2)_3-PPh_2Ni(CO)_2PPh_3$ and $\{Si\}-O-(CH_2)_3-PPh_2RhCl(CO)PPh_3$ were grown on the ⟨111⟩ surface of the single-side polished Si wafers. A KRS crystal was sandwiched between the reflective faces of two silicon wafers, and the angle of the incident light (θ) was set
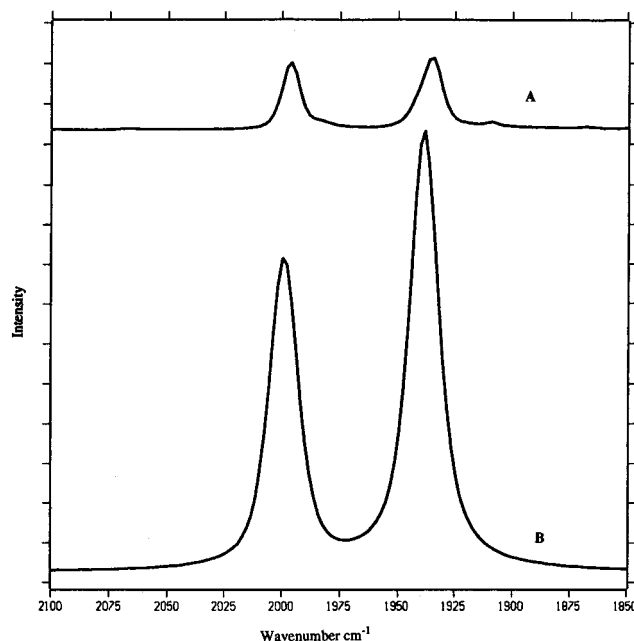
Figure 1. FT-IR-ATR spectrum (1850−2100 cm^{-1} region) of a thin film of $[Si]-O-(CH_2)_3PPh_2Ni(CO)_2PPh_3$ (A) on a single-crystal silicon wafer (one side polished), and FT-IR spectrum (1850−2100 cm^{-1} region) of $(CH_3)_3Si-O-(CH_2)_3-PPh_2Ni(CO)_2PPh_3$ in Nujol (B).

at 45° at a resolution of 2 cm^{-1}. The FT-IR-ATR spectrum of the thin film, $\{Si\}-O-(CH_2)_3-PPh_2Ni-(CO)_2PPh_3$ on single-crystal Si (A) and an FT-IR spectrum of $(CH_3)_3Si-O-(CH_2)_3-PPh_2Ni(CO)_2PPh_3$ in Nujol (B) are shown in Figure 1. The similarities in ν_{CO} stretching frequencies between the IR spectra of the solution model and the supported metal complex indicate that the complexes are electronically unchanged when bound to the silylated surface. The monolayer structure on the flat silicon wafer produces two ν_{CO} stretching frequencies which are of roughly equal intensities.[21a] The intensity and the number of bands
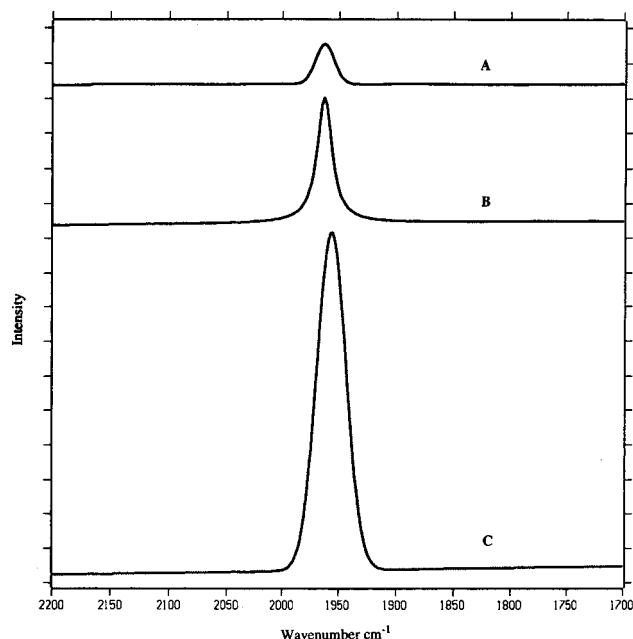
Figure 2. FT-IR-ATR spectrum (1700−2200 cm^{-1} region) of a thin film of [Si]−O−(CH$_2$)$_3$PPh$_2$RhCl(CO)PPh$_3$ (A) on a single-crystal silicon wafer (one side polished), and FT-IR spectrum (1700−2200 cm^{-1} region) of (CH$_3$)$_3$Si−O−(CH$_2$)$_3$PPh$_2$RhCl(CO)PPh$_3$ in Nujol (B).

in the FT-IR spectrum depend on the symmetry of the molecule.[21b] For the complex in solution, two unequal carbonyl stretching frequencies are due to the symmetric and asymmetric dipole moment changes in the tetrahedral Ni(0) complex. Since the intensities of the carbonyl stretching frequencies are equivalent for the surface-bound complex, it might suggest that due to the packing arrangement in the thin film, the Ni complex is forced to orient itself in a distorted tetrahedral geometry.

The thin film of {Si}−O−(CH$_2$)$_3$−PPh$_2$RhCl(CO)PPh$_3$ on single-crystal silicon showed a single ν_{CO} stretching frequency at 1964 cm^{-1} in its FT-IR-ATR spectrum (Figure 2) which is identical to its solution analogue (CH$_3$)$_3$Si−O−(CH$_2$)$_3$−PPh$_2$RhCl(CO)PPh$_3$ (ν_{CO} = 1964 cm^{-1}). The FT-IR-ATR spectra of these thin films also depict the asymmetric stretching mode of the alkyl chain in the above complex at 2950 cm^{-1} and the phenyl stretching mode at 3039 cm^{-1}.

Catalytic Oligomerization of Phenylacetylene. It is well-known that phenylacetylene can be oligomerized using a Ni(0) catalyst, Ni(CO)$_2$(PPh$_3$)$_2$, in a monomer-to-catalyst ratio of 250:1, resulting in cyclic and linear trimeric products, 1,2,4-triphenylbenzene (70%), 1,3,6-triphenyl-1-yne-3,5-diene (30%), and 1,3,5-triphenylbenzene (in less than 1% yield).[22a,e] To accurately compare the catalytic properties of the thin film [Si]−O−(CH$_2$)$_3$PPh$_2$Ni(CO)$_2$PPh$_3$ with a solution model complex, we carried out oligomerization of phenylacetylene

using the solution model complex Ni(CO)$_2$(PPh$_3$)-[PPh$_2$(CH$_2$)$_3$OSi(CH$_3$)$_3$] in monomer-to-catalyst ratios of 250:1 and 24000:1. The latter ratio is approximately equal to the catalyst concentration of the covalently anchored organometallic complex on a 1 in. × 1 in. glass slide. Similar to earlier studies,[22a,e] both solution reactions resulted in the formation of 1,2,4-triphenylbenzene as the major product and 1,3,6-triphenyl-1-yne-3,5-diene and 1,3,5-triphenylbenzene as the minor products. Although the product distributions are similar, the most significant difference is in their catalytic efficiencies. The monomer-to-catalyst ratio of 24000:1 was found to be highly inefficient in oligomerizing phenylacetylene. This study indicates that the polymerization of phenylacteylene diminishes significantly between the ratios of 250:1 to 24000:1, as suggested earlier by Meriwether.[22e]

A similar catalytic reaction using a thin film of [Si]−O−(CH$_2$)$_3$PPh$_2$−Ni(CO)$_2$PPh$_3$ supported on a 1 in. × 1 in. glass slide produced a mixture with a product distribution of symmetric 1,3,5-triphenylbenzene at 56%, the unsymmetrical 1,2,4-triphenylbenzene at 23%, and a linear isomer 1,4,6-triphenyl-1-yne-3,5-diene at 21%. This is considerably different from the product distribution in the homogeneous catalysis and suggests selectivity of the surface-immobilized Ni complex in the oligomerization of phenylacetylene. The turnover efficiency of the catalyst, which was determined based on the concentration of the Ni complex found experimentally by UV−vis absorption spectroscopy, was found to be 1656 h^{-1}.[15e,23] The turnover rate of the cyclooligomerization using the Ni complex in solution with a monomer-to-catalyst ratio similar to the surface reaction was found to be 1.16 × 10^{-3} h^{-1}. Although one should be cautious in comparing surface turnover efficiency, which is based on the concentration of catalyst estimated from UV−vis spectra, with the turnover rate in solution, it seems that the catalytic activity is significantly enhanced upon supporting the complex on glass. This suggests that the support may not be merely an inert backbone but may take a positive role in promoting catalyst activity and selectivity.

A detailed examination[22a,e] of the polymerization reaction of numerous acetylenes with Ni(CO)$_2$(PPh$_3$)$_2$ in solution has established that the "active catalyst" in these reactions is obtained by the loss of both CO ligands followed by a possible oxidative addition of acetylene to this Ni(0) coordinatively unsaturated complex. As discussed above, polymerization of phenylacetylene with the surface-anchored [Si]−O−(CH$_2$)$_3$PPh$_2$Ni(CO)$_2$PPh$_3$ complex afforded a different product ratio than a similar reaction in solution with Ni(CO)$_2$(PPh$_3$)$_2$ or Me$_3$SiO−(CH$_2$)$_3$−PPh$_2$Ni(CO)$_2$(PPh$_3$). We were intrigued by the possibility of an alternative pathway which may be operative in the former reaction. To evaluate this hypothesis, we undertook a time-evolved FT-IR study of this reaction. The Ni(0) complex was supported on a

(21) (a) The peak integration analysis was performed using an OPUS V2.2 program and Levenberg−Marquardt algorithm: Ni(CO)$_2$(PPh$_3$)-(PPh$_2$(CH$_2$)$_3$OSiMe$_3$), ν_{CO} 1938 (intensity = 0.1992, width = 15.529, and integral = 4.554), ν_{CO} 1999 (intensity = 0.1408, width = 14.973, and integral = 2.923); [Si]−O−(CH$_2$)$_3$PPh$_2$Ni(CO)$_2$PPh$_3$ ν_{CO} 1936 (intensity = 0.1964, width = 12.599, and integral = 2.634), ν_{CO} 1996 (intensity = 0.1968, width = 8.980, and integral = 2.416). (b) Cotton, F. A.; Wilkinson, G. *Advanced Inorganic Chemistry*, 3rd ed., Interscience Publishing: New York, 1972; pp 695−697.

(22) (a) Meriwether, L. S.; Colthup, E. C.; Kennerly, G. W.; Reusch, R. N. *J. Org. Chem.* **1961**, *26*, 5155. (b) Heimback, P.; Jolly, P. W.; Wilke, G. *Adv. Organomet. Chem.* **1970**, *8*, 29. (c) Semmelhack, M. F. *Org. React.* **1972**, *19*, 115. (d) Heimback, P. *Angew. Chem., Int. Ed. Engl.* **1973**, *12*, 975. (e) Meriwether, L. S.; Colthup, E. C.; Kennerly, G. W.; Leto, M. F. *J. Org. Chem.* **1962**, *27*, 3930.

(23) Turnover efficiency was determined using the surface coverage estimated from UV−vis absorption spectroscopy: 3 × 10^{-9} mol cm^{-2} × 6.25 cm^2 × 2 = 3.75 × 10^{-8} mol of Ni complex present on both sides of the glass slide: 2.4837 × 10^{-4} mol of product/3.75 × 10^{-8} mol of Ni catalyst/4 h = 1656 h^{-1}.

Table 5.   XPS^a of Thin Films of [Si]−O−(CH$_2$)$_3$PPh$_2$Ni(CO)$_2$PPh$_3$ Before (1) and After (2) the Catalytic Cycle

element	binding energy (eV)	FWHM	Concs. (%)^b	peak area	$I_x/S_x{}^c$	$C_x{}^d$
			Thin Film **1**			
Ni2p$_{3/2}$	855.0	9.00	6.95	242 257.27	80 752.425	0.1527
O1s	533.0	7.00	17.62	60 067.747	91 011.738	0.1721
C1s	286.0	6.00	60.25	50 794.174	203 176.699	0.3842
P2p$_{3/2}$	132.0	8.00	6.27	38 113.875	105 871.876	0.2002
Si2p	103.0	6.00	8.91	12 964.81	48 017.810	0.0908
			Thin Film **2**			
Ni2p$_{3/2}$	858.0	10.00	4.71	106 187.399	35 395.797	0.1189
O1s	534.0	8.00	22.59	48 210.465	73 046.159	0.2453
C1s	288.0	6.00	57.26	26 478.846	105 915.384	0.3557
P2p$_{3/2}$	134.0	8.00	4.14	15 631.952	43 422.089	0.1458
Si2p	102.0	6.00	11.30	10 805.510	40 020.407	0.1344

^{a} XPS carried out on VG Escalab MKII instrument using Mg Kα radiation. ^{b} Calculation of peak areas and integration performed using the program Surfsoft version 1.4. ^{c} I_x/S_x = peak area/atomic sensitivity factor. ^{d} Integration: $C_x = [I_x/S_x]/[\sum I_i/S_i]$.
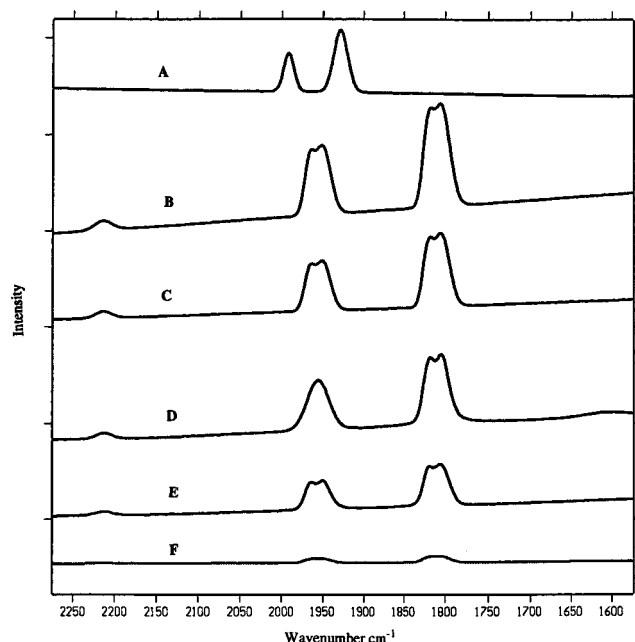
Figure 3. FT-IR spectra (1575−2275 cm^{-1} region) of a thin film of [Si]−O−(CH$_2$)$_3$PPh$_2$Ni(CO)$_2$PPh$_3$ on a borosilicate glass slide (thickness = 0.16 mm) at time (t) = 0 (A), 15 (B), 30 (C), 60 (D), 120 (E), and 240 min (F).

thin glass slide (24 × 24 mm, 0.16 nm thick) using the deposition chemistry described above. Unfunctionalized glass slides of such thickness are transparent in the IR region of interest and are invaluable in monitoring surface reactions. The FT-IR spectra of a thin film of {Si}−O−(CH$_2$)PPh$_2$Ni(CO)$_2$PPh$_3$ before placing it in the reaction mixture (A) and after 15 (B), 30 (C), 60 (D), 120 (E) and 240 (F) min of its reaction with phenylacetylene at 90 °C in benzene are shown in Figure 3. As expected, a thin film of {Si}−O−(CH$_2$)$_3$PPh$_2$Ni-(CO)$_2$PPh$_3$ before any reaction shows two ν_{CO} stretching frequencies at 1996 and 1935 cm^{-1}. The most significant changes in the FT-IR spectra take place after 15 min of the reaction (B), where the original peaks are replaced with the peaks at 3102 (br), 3049 (br), 2210 (w, br), 1967 and 1954 (s, br), and 1812 (br) cm^{-1} (Figure 3). It indicates that during this time, the active catalyst is formed on the surface which proceeds with the oligomerization of phenylacetylene. The above peaks in the FT-IR spectra may be assigned as follows: 3102 and 3049 cm^{-1} to the aromatic ring and 2210 ($\nu_{C\equiv C}$), 1967 Ni−H, 1954 (ν_{CO}), and 1812 cm^{-1} to the π-bound phenylacetylene. These observations suggest that there

may be an initial loss of a triphenylphosphine and a carbonyl ligand from the surface-bound {Si}−O−(CH$_2$)$_3$PPh$_2$Ni(CO)$_2$PPh$_3$ complex, followed by attack with phenylacetylene. Anchoring of the Ni complex to the surface may create a specific environment almost like a reactive pocket where, for steric reasons, the addition of phenylacetylene occurs in an orientation that favors the formation of symmetric 1,3,5-triphenylbenzene.

XPS Study of Thin Films of [Si]−O−(CH$_2$)$_3$PPh$_3$-Ni(CO)$_2$PPh$_3$ Before and After Catalysis. A quantitative evaluation of the thin films of [Si]−O−(CH$_2$)$_3$-PPh$_2$Ni(CO)$_2$PPh$_3$ before and after catalysis using XPS was undertaken in order to establish whether there is any leaching of the Ni complex during the catalytic process. Two different slides from the same batch were used for this experiment. Table 5 contains the XPS data including peak positions, concentrations, and integrations of each element present on the surface before and after catalysis.

The Ni 2p$_{3/2}$, P 2p$_{3/2}$, and C 1s peaks show a decrease in atomic concentration by 32%, 34%, and 5%, respectively. The O 1s and Si 2p atomic concentration increased by 22% and 21%. The relative integration of the Ni peak similarly results in a decrease from 0.1527 to 0.1189. A decrease in peak integration is likewise seen for the phosphorus and carbon peaks, and the silicon and oxygen peaks showed an increase in their integration. In addition to the possibility of leaching of the Ni complex during the catalytic cycle, we must also take into account varying degrees of radiation damage which could cause peak intensities to diminish. The peak positions of Ni, P, and C are also shifted to higher binding energies, which suggests that these elements are not in the same environment as they were prior to the catalytic reaction. As discussed above, a carbonyl and a phosphine ligand may have been lost in the formation of the active catalyst, resulting in the modification of the electronics at the metal center. This is perhaps also the reason for the 3 eV shift in the Ni 2p$_{3/2}$ binding energy. There is also an increase in the C 1s binding energy, which suggests the presence of an unsatured carbon center.

Conclusions

The new surface modification technique based on simple acid−base hydrolytic chemistry is a versatile approach to functionalize inorganic oxide surfaces under

mild reaction conditions and using commercially available reagents. Compared with the original silane condensation methods, this deposition process leads to phosphine-oxide-free thin films when tertiary phosphines are employed as chromophores. These thin films containing amine and phosphine donor ligands covalently bind a variety of transition-metal complexes. Characterization of the bound species by a variety of techniques has helped evaluate their actual environment on the surface. Such a thin film of a Ni(0) complex, $[Si]-O(CH_2)_3PPh_2-Ni(CO)_2PPh_3$, on glass oligomerizes phenylacetylene with a product ratio that is different from that of its solution analogues, $(CH_3)_3Si-O(CH_2)_3PPh_2-Ni(CO)_2PPh_3$ and $Ni(CO)_2(PPh_3)_2$. Evaluation of this catalytic reaction suggests that the formation of the products can be explained by considering an initial loss of a phosphine and a carbonyl ligand, instead of the loss of both carbonyl ligands in the catalytic reaction in solution. Thus, catalytic activity and selectivity can be enhanced by anchoring organometallic complexes on flat surfaces, leading to tailored metal catalysis by molecular self-assembly. We are currently evaluating the role of this type of molecular order in catalysis.

Experimental Section

Materials and Measurements. All experiments were performed using appropriately sized Schlenk flasks and molecular self-assembly apparatus, under a nitrogen atmosphere. Toluene, benzene, THF, diethyl ether, and hexanes were stored under nitrogen after being distilled over sodium. Diethylamine, 3-(diethylamino)-1-propanol, and 5-(diethylamino)-2-pentanol were dried over KOH and distilled prior to use. NMR spectra were recorded on either a Gemini 200 MHz or a JEOL 270 MHz spectrometer. All NMR samples were prepared under a nitrogen atmosphere in either C_6D_6 or $CDCl_3$. Chemical shifts reported are relative to tetramethylsilane as an internal standard for ^1H NMR spectra and to H_3PO_4 for ^{31}P-$\{^1H\}$ NMR spectra. Electron impact (EI) and fast atom bombardment (FAB) mass spectra were obtained using a low-resolution KRATOS MS25RSA spectrometer with xenon as the ionizing gas and nitrobenzyl alcohol as the matrix. Elemental analyses were performed by either Microanalytical Service Ltd. (Chemical Engineering), Montreal, Quebec, or Guelph Chemical Laboratories Ltd., Guelph, Ontario. Gas chromatography analysis was performed on a Hewlett-Packard 6840 instrument using He as the carrier gas. Samples for GC-MS were analyzed on a Hewlett-Packard 5988A instrument using He as the carrier gas, with an injector temperature of 250 °C, source temperature of 200 °C, and electron-impact energy of 70 eV at 300 μA trap current.

The static contact angles for the thin films were measured using a Rame-Hart NRL100 goniometer using deionized water and hexadecane as probe liquids. X-ray photoelectron spectra were measured either on a INRS 220i XL spectrometer, Varenne, Quebec, or on a VG Escalab MKII instrument, École Polytechnique, Université de Montreal. Binding energies, peak intensities, and peak widths at half-height were recorded using Al Kα or Mg Kα radiation to produce the photoemission of electrons from the core levels of the surface atoms. About 60 Å of depth was probed for a detector perpendicular to the surface. The analyzed surface was 2×3 mm. All peak positions were corrected for carbon at 285.0 eV in binding energy to adjust for charging effects. The power of the source was 300 W and a pressure of 1×10^{-9} Torr. Lines were measured for Si $2p_{1/2}$, O 1s, C 1s, P 2s, P $2p_{3/2}$, N 1s, Cl 2s, Ni $2s_{1/2}$, Ni $2p_{3/2}$, Rh $3d_{5/2}$, and Pd $3d_{5/2}$. Air-sensitive films were usually run a number of times, attempting to minimize the intensity of the O 1s line, the line widths of the P 2s, Ni 2s, and Rh $3d_{5/2}$ lines, and the base line slope in the Ni 2s region. The solid-state $^{31}P\{^1H\}$ NMR spectra were recorded on a Chemagnetics CMX-300 MHz spectrometer using ammonium phosphate as an internal standard and operating at 121.279 MHz, with high-power decoupling, using a recycle time of 6 s and a contact time of 2 ms. Different spinning rates, ranging from 1.5 to 4.5 kHz, were used to identify the isotropic peaks. Calculation of the shielding tensors was achieved with the aid of a computational package developed by Kentgens et al.[24] Infrared spectra were recorded on a Bruker IFS-48 Fourier transform infrared spectrophotometer using a standard resolution of 4 cm^{-1} for transmission and 2 cm^{-1} for attenuated total reflection experiments. The organometallic thin films were studied using FT-IR in the transmission and ATR modes, and in the latter case, a KRS crystal was placed between the reflective sides of ⟨111⟩ Si wafers. A miniature pressure device was employed in order to maximize optical contact. A critical incidence angle of $\theta = 45°$ was used, since this geometry yields a maximum signal of 6000 counts/s.

Preparation of Solution Models: $(CH_3)_3SiOC_6H_4N$-$(C_2H_5)_2$ (1). 3-(Diethylamino)phenol (87.4 mg, 0.53 mmol) was dissolved in toluene (30 mL) to which $(CH_3)_3Si-N(C_2H_5)_2$ (100 μL, 0.53 mmol) was added. The mixture was stirred at room temperature for 18 h under an atmosphere of N_2. There was a distinct color change from deep brown to red. Removing the solvent under vacuum gave a red oily product. Yield: 0.12 g (96%). ^1H NMR (C_6D_6, 270 MHz): δ 0.10 (9H, s, $(CH_3)_3Si$), 0.89 (6H, t, $J_{H-H} = 7$ Hz, NCH_2CH_3), 2.97 (4H, q, $J_{H-H} = 7.2$ Hz, N$-CH_2$), 6.29, 6.39, 7.09 (4H, m, C_6H_4-N). EI-MS: m/z 237. Anal. Calcd for $C_{13}H_{23}NOSi$ (237.4): C, 65.77; H, 9.76; N, 5.89. Found: C, 65.45; H, 9.79; N, 5.88.

$(CH_3)_3SiO(CH_2)_3N(C_2H_5)_2$ (2). To a solution of 3-(diethylamino)-1-propanol (78.5 μL, 0.53 mmol) in 20 mL of benzene, $(CH_3)_3Si-N(C_2H_5)_2$ (100 μL, 0.53 mmol) was added, resulting in an immediate color change from colorless to yellow. The mixture was allowed to stir at room temperature for 10 h. The solvent and diethylamine were distilled, leaving behind a yellow oil with a yield of 0.11 mL (90%). ^1H NMR (C_6D_6, 270 MHz): δ 0.09 (9H, s, $(CH_3)_3Si$), 0.86 (6H, t, $J_{H-H} = 7.2$ Hz, CH_3CH_2N), 1.65 (2H, m, $J_{H-H} = 7$ Hz, $CH_2CH_2CH_2$), 2.19 (4H, q, $J_{H-H} = 7.2$ Hz, N$-CH_2CH_3$), 2.26 (2H, t, $J_{H-H} = 6$ Hz, N$-CH_2$), 3.79 (2H, t, $J_{H-H} = 6.5$ Hz, O$-CH_2$). EI-MS: m/z 203. Anal. Calcd for $C_{10}H_{25}SiON$ (203.4): C, 59.05; H, 12.39; N, 6.88. Found: C, 58.76; H, 11.77; N, 7.01.

$(CH_3)_3SiOCH(CH_3)(CH_2)_3N(C_2H_5)_2$ (3). To a solution of 5-(diethylamino)-2-pentanol (97.3 μL, 0.53 mmol) in benzene (20 mL), $(CH_3)_3Si-N(C_2H_5)_2$ (100 μL, 0.53 mmol) was added, and the mixture was left to stir at room temperature for 24 h. The solvent and diethylamine were distilled in vacuo, affording a yellow oil. Yield: 0.10 mL (82%). ^1H NMR (C_6D_6, 270 MHz): δ 0.11 (9H, s, $(CH_3)_3Si$), 0.88 (6H, t, $J_{H-H} = 7.2$ Hz, N$-CH_2CH_3$), 1.27 (3H, d, $J_{H-H} = 6.8$ Hz, CH(CH_3)), 1.38 (2H, m, $J_{H-H} = 6.8$ Hz, $CH_2CH_2CH_2$), 1.55 (2H, t, $J_{H-H} = 6.4$ Hz, N$-CH_2CH_2$), 2.16 (4H, q, $J_{H-H} = 6.5$ Hz, N$-CH_2CH_3$), 2.35 (2H, q, $J_{H-H} = 6.7$ Hz, $CH_2CH(CH_3)$), 3.73 (1H, m, $J_{H-H} = 6.9$ Hz, $CH(CH_3)$). EI-MS: m/z 231. Anal. Calcd for $C_{12}H_{29}SiON$ (231.45): C, 62.27; H, 12.63; N, 6.05. Found: C, 62.63; H, 12.83; N, 6.24.

$(CH_3)_3SiO(CH_2)_4P(C_2H_5)_2$ (4). A mixture of (4-hydoxybutyl)diethylphosphine (100 mg, 0.62 mmol) and $(CH_3)_3Si-N(C_2H_5)_2$ (117 μL, 0.62 mmol) in 25 mL of benzene were stirred at room temperature for 21 h. Diethylamine and benzene were distilled under vacuum, resulting in a pale yellow oil. Yield: 0.13 mL (94%). ^1H NMR (C_6D_6, 270 MHz): δ 0.09 (9H, s, $(CH_3)_3Si$), 0.95 (4H, m, $J_{H-H} = 7$ Hz, CH_2CH_2), 1.19 (6H, t,

(24) Kentgens, A. P.; Power, W.; Wasylishen, R. E. *HBLQFIT Sideband Analysis*, version 2.2; Dalhousie University: Halifax, Nova Scotia, Canada, 1991.

J_{H-H} = 8 Hz, PCH$_2$CH_3), 1.56 (2H, m, J_{H-H} = 7 Hz, PCH_2-CH$_2$), 2.48 (4H, q, J_{H-H} = 8 Hz, PCH_2CH$_3$), 3.50 (2H, t, J_{H-H} = 6 Hz, O−CH_2). ^{31}P{^{1}H} (C$_6$D$_6$, 270 MHz): δ −21.7 (s). EI-MS: *m/z* 234. Anal. Calcd for C$_{11}$H$_{27}$POSi (234.4): C, 56.37; H, 11.61. Found: C, 56.18; H, 11.72.

(CH$_3$)$_3$SiO(CH$_2$)$_3$P(C$_6$H$_5$)$_2$ (5). (3-Hydroxypropyl)diphenylphosphine (55 mg, 0.23 mmol) was dissolved in benzene (25 mL), and (CH$_3$)$_3$Si−N(C$_2$H$_5$)$_2$ (42.6 μL, 0.23 mmol) was added. The mixture was stirred at room temperature for 22 h under a stream of N$_2$. Distillation in vacuo afforded a colorless oil. Yield: 0.065 mL (91.5%). ^{1}H NMR (C$_6$D$_6$, 200 MHz): δ 0.09 (9H, s, (CH_3)$_3$Si), 1.72 (2H, m, J_{H-H} = 6 Hz, CH$_2$CH_2CH$_2$), 2.09 (2H, m, J_{H-H} = 6 Hz, P−CH_2), 3.52 (2H, t, J_{H-H} = 6 Hz, O−CH_2), 7.10, 7.46 (10H, m (br), P(C$_6$H$_5$)$_2$). ^{31}P{^{1}H} (C$_6$D$_6$, 270 MHz): δ −14.05 (s). EI-MS: *m/z* 316. Anal. Calcd for C$_{18}$H$_{25}$POSi (316.45): C, 68.32; H, 7.96. Found: C, 68.31; H, 7.88.

(CH$_3$)$_3$SiOC$_6$H$_4$P(C$_6$H$_5$)$_2$ (6). To a solution of (2-hydroxyphenyl)diphenylphosphine (35 mg, 0.124 mmol) in 10 mL of benzene, (CH$_3$)$_3$Si−N(C$_2$H$_5$)$_2$ (23 μL, 0.124 mmol) was added, and the mixture was stirred at ambient temperature for 24 h under nitrogen. The solvent and diethylamine were distilled off under vacuum to give a pale yellow oil. Yield: 0.04 mL, (91%). ^{1}H NMR (C$_6$D$_6$, 200 MHz): δ 0.06 (9H, s, (CH_3)$_3$Si), 6.70, 7.05, 7.88 (14H, m, C$_6$H$_4$P(C$_6$H$_5$)$_2$). ^{31}P{^{1}H} (270 MHz, C$_6$D$_6$): δ 25.6 (s). EI-MS: *m/z* 351. Anal. Calcd for C$_{21}$H$_{23}$-POSi (350.5): C, 71.97; H, 6.61. Found: C, 71.80; H, 6.42.

[(CH$_3$)$_3$SiO(CH$_2$)$_3$P(C$_6$H$_5$)$_2$]Ni(CO)$_2$P(C$_6$H$_5$)$_3$ (7). Ni(CO)$_2$-(P(C$_6$H$_5$)$_3$)$_2$ (0.20 g, 0.31 mmol) was dissolved in 20 mL of toluene to which 100 μL (0.31 mmol) of **5** was added, and the mixture was set to reflux at 90 °C for 21 h. The solvent was evaporated to dryness under vacuum, and the pale yellow residue was washed with diethyl ether (10 mL), followed by recrystallization from a toluene/hexane mixture to give a pale yellow flaky solid. Yield: 0.20 g (91%). ^{1}H NMR (270 MHz, C$_6$D$_6$): δ 0.07 (9H, s, (CH_3)$_3$Si), 1.71 (2H, m, J_{H-H} = 5 Hz, CH$_2$CH_2CH$_2$), 2.10 (2H, t, J_{H-H} = 5 Hz, OCH_2), 3.52 (2H, t, J_{H-H} = 5 Hz, OCH_2), 7.07, 7.41 (10H, m, P(C$_6$H$_5$)$_2$), 7.32, 7.87 (15H, m, P(C$_6$H$_5$)$_3$). ^{31}P{^{1}H} NMR (C$_6$D$_6$, 270 MHz): δ 34.0 (d, J_{P-P} = 82 Hz), 25.1 (d, J_{P-P} = 82 Hz). IR (Nujol): ν_{CO} 1999, 1938 cm^{-1}. EI-MS: *m/z* 693. Anal. Calcd for C$_{38}$H$_{40}$O$_3$P$_2$SiNi (693.46): C, 65.82; H, 5.81. Found: C, 66.57; H, 5.89.

[(CH$_3$)$_3$SiO(CH$_2$)$_4$P(C$_2$H$_5$)$_2$]Ni(CO)$_2$(P(C$_6$H$_5$)$_3$) (8). A mixture of Ni(CO)$_2$(P(C$_6$H$_5$)$_3$)$_2$ (273 mg, 0.43 mmol) and compound **4** (100 μL, 0.43 mmol) in 25 mL of toluene was set to reflux at 80 °C for 24 h. The solvent was evaporated to dryness under vacuum, and the beige residue was crystallized from a toluene/hexane mixture affording a beige powder. Yield: 248 mg (95%). ^{1}H NMR (270 MHz, C$_6$D$_6$): δ 0.12 (9H, s, (CH_3)$_3$Si), 0.83 (4H, m, J_{H-H} = 7.2 Hz, CH_2CH_2), 1.21 (6H, t, J_{H-H} = 6.9 Hz, PCH$_2$CH_3), 1.57 (2H, m, J_{H-H} = 6.8 Hz, PCH_2CH$_2$), 3.24 (4H, q, J_{H-H} = 6.9 Hz, PCH_2CH$_3$), 3.66 (2H, t, J_{H-H} = 7 Hz, OCH_2), 7.42, 7.68 (15H, m, P(C$_6$H$_5$)$_3$). ^{31}P{^{1}H} NMR (270 MHz, C$_6$D$_6$): δ 27.1 (d, J_{P-P} = 75 Hz), 26.3 (d, J_{P-P} = 75 Hz) ppm. IR (Nujol): ν_{CO} 1996, 1934 cm^{-1}. EI-MS: *m/z* 614. Anal. Calcd for C$_{31}$H$_{42}$O$_3$P$_2$SiNi (611.4): C, 60.90; H, 6.92. Found: C, 60.23; H, 6.19. XPS (Al Kα): Si (2p, 98 eV), P (2s, 188 eV), C (1s, 280 eV), O (1s, 531 eV), Ni (2p, 852 eV).

[(CH$_3$)$_3$SiN(C$_2$H$_5$)$_2$]Ni(CO)$_2$P(C$_6$H$_5$)$_3$ (9). Ni(CO)$_2$(P(C$_6$H$_5$)$_3$)$_2$ (0.250 g, 0.39 mmol) and (CH$_3$)$_3$SiN(C$_2$H$_5$)$_2$ (74 μL, 0.39 mmol) were dissolved in 30 mL of toluene. The mixture was stirred for 2 h at room temperature and was then set to reflux at 70 °C for 18 h. The solvent was concentrated to 5 mL and layered with hexane. A white solid precipitated, which was filtered and dried under vacuum. Yield: 185 mg (91%). ^{1}H NMR (270 MHz, C$_6$D$_6$): δ 0.11 (9H, s, (CH_3)$_3$Si), 1.12 (6H, t, J_{H-H} = 7 Hz, NCH$_2$CH_3), 3.02 (4H, q, J_{H-H} = 7 Hz, NCH_2CH$_3$), 7.05, 7.87 (15H, m, P(C$_6$H$_5$)$_3$). ^{31}P{^{1}H} NMR (270 MHz, C$_6$D$_6$): δ 27.3 (s). IR (Nujol): ν_{CO} 1981, 1934 cm^{-1}. EI-MS: *m/z* 522. Anal. Calcd for C$_{27}$H$_{34}$O$_2$NPSiNi (522.3): C, 62.09; H, 6.56; N, 2.68. Found: C, 61.05; H, 6.05; N, 2.66.

[(CH$_3$)$_3$SiO(CH$_2$)$_3$N(C$_2$H$_5$)$_2$]Ni(CO)$_2$(P(C$_6$H$_5$)$_3$) (10). Ni-(CO)$_2$(P(C$_6$H$_5$)$_3$)$_2$ (208 mg, 0.33 mmol) and compound **2** (75 μL, 0.33 mmol) were dissolved in toluene (20 mL), and the mixture was set to reflux at 85 °C for 14 h. The solution was evaporated to dryness under vacuum, and the pale yellow residue was washed with 20 mL of diethyl ether to give a pale yellow flaky solid. Yield: 170 mg (90.4%). ^{1}H NMR (270 MHz, C$_6$D$_6$): δ 0.15 (9H, s, (CH_3)$_3$Si), 1.06 (6H, t, J_{H-H} = 8 Hz, NCH$_2$CH_3), 1.78 (2H, m, J_{H-H} = 7.8 Hz CH$_2$CH_2CH$_2$), 2.56 (4H, q, J_{H-H} = 8 Hz, NCH_2CH$_3$), 3.39 (2H, t, J_{H-H} = 7.9 Hz, NCH_2-CH$_2$), 4.72 (2H, t, J_{H-H} = 8 Hz, OCH_2), 7.25, 7.80 (15H, m, P(C$_6$H$_5$)$_3$). ^{31}P{^{1}H} NMR (270 MHz, C$_6$D$_6$): δ 26.7 (s). IR (Nujol): ν_{CO} 1982, 1936 cm^{-1}. Anal. Calcd for C$_{30}$H$_{40}$O$_3$NPSiNi (580.40): C, 62.08; H, 6.94; N, 2.41. Found: C, 62.65; H, 6.65; N, 2.46. ^{31}P{^{1}H} NMR (cross polarization): δ 28.3 (s). XPS (Al Kα): Si (2p, 97 eV), P (2s, 192 eV), C (1s, 280 eV), O (1s, 528 eV), N (2s, 394 eV), Ni (2p, 850 eV).

[(CH$_3$)$_3$SiOCH(CH$_3$)(CH$_2$)$_3$N(C$_2$H$_5$)$_2$]Ni(CO)$_2$P(C$_6$H$_5$)$_3$ (11). To a solution of **3** (75 μL, 0.28 mmol) in 25 mL of toluene, Ni-(CO)$_2$(P(C$_6$H$_5$)$_3$)$_2$ (179 mg, 0.28 mmol) was added, and the mixture was allowed to reflux at 70 °C for 15 h under an atmosphere of nitrogen. The solvent was evaporated under vacuum, and the pale yellow residue was recrystallized from a toluene/hexane mixture to yield a pale yellow solid. Yield: 155 mg (91%). ^{1}H NMR (270 MHz, C$_6$D$_6$): δ 0.12 (9H, s, (CH_3)$_3$-Si), 0.80 (6H, t, J_{H-H} = 8 Hz, NCH$_2$CH_3), 1.25 (3H, d, J_{H-H} = 7 Hz, CH(CH_3)), 1.36 (2H, m, J_{H-H} = 7 Hz, CH$_2$CH_2CH$_2$), 2.20 (4H, q, J_{H-H} = 6 Hz, NCH_2CH$_3$), 2.40 (2H, m, J_{H-H} = 6.5 Hz, CH_2CH(CH$_3$)), 3.20 (2H, t, J_{H-H} = 6 Hz, CH$_2$CH_2N), 3.70 (1H, m, (CH$_3$)CH), 7.24, 7.92 (15H, m, P(C$_6$H$_5$)$_3$). ^{31}P{^{1}H} NMR (270 MHz, C$_6$D$_6$): δ 26.9 (s). IR (Nujol): ν_{CO} 1975, 1916 cm^{-1}. EI-MS: *m/z* 609. Anal. Calcd for C$_{32}$H$_{44}$O$_3$PNSiNi (608.44): C, 63.17; H, 7.29; N, 2.30. Found: C, 63.39; H, 7.15; N, 2.09. Solid-state ^{31}P{^{1}H} NMR (cross polarization): δ 31.1 (s). XPS (Al Kα): Si (2p, 97 eV), P (2s, 192 eV), C (1s, 279 eV), O (1s, 527 eV), N (2s, 394 eV), Ni (2p, 849.0 eV).

[(CH$_3$)$_3$SiO(CH$_2$)$_3$P(C$_6$H$_5$)$_2$]RhCl(CO)(P(C$_6$H$_5$)$_3$) (12). To a solution of RhCl(CO)(P(C$_6$H$_5$)$_3$)$_2$ (50 mg, 0.072 mmol) in benzene (20 mL), compound **5** (23 μL, 0.072 mmol) was added, and the mixture was heated to 50 °C for 20 h. The solvent was evaporated to dryness under vacuum to afford a yellow residue, which was washed with ether (10 mL) and hexane (15 mL) and then dried under vacuum. Yield: 38 mg (73%). ^{1}H NMR (270 MHz, C$_6$D$_6$): δ 0.06 (9H, s, (CH_3)$_3$Si), 1.76 (2H, m, J_{H-H} = 6.7 Hz, CH$_2$CH_2CH$_2$), 2.28 (2H, m, J_{H-H} = 7.2 Hz, PCH_2), 3.51 (2H, t, J_{H-H} = 6 Hz, OCH_2), 7.37, 7.73 (10H, m, P(C$_6$H$_5$)$_2$), 7.07, 7.52 (15H, m, P(C$_6$H$_5$)$_3$). ^{31}P{^{1}H} NMR (270 MHz, C$_6$D$_6$): δ 24.4 (d, J_{Rh-P} = 116 Hz), 23.7 (d, J_{Rh-P} = 116 Hz). IR (Nujol): ν_{CO} 1964 cm^{-1}. FAB-MS: *m/z* 754. Anal. Calcd for C$_{37}$H$_{40}$O$_2$P$_2$ClSiRh (745.11): C, 59.64; H, 5.41. Found: C, 61.35; H, 5.52. ^{31}P{^{1}H} NMR (cross polarization): δ 27.5 (d), 23.4 (d). XPS (Al Kα): Si (2p, 97 eV), P (2s, 192 eV), C (1s, 281 eV), O (1s, 528 eV), Cl (2s, 269 eV), Rh (3d, 309 eV).

[(CH$_3$)$_3$SiO(CH$_2$)$_3$P(C$_6$H$_5$)$_2$]Rh(CO)$_2$Cl (13). A 20 mg solution of [Rh(CO)$_2$Cl]$_2$ (0.051 mmol) and compound **5** (32 μL, 0.102 mmol) was dissolved in benzene (15 mL). There was an immediate color change from red to yellow. The mixture was left to stir at room temperature for 3 h under an atmosphere of nitrogen. The solvent was evaporated to dryness under vacuum to leave behind a bright yellow residue, which was recrystallized from a toluene/hexane mixture. Yield: 25 mg (96%). ^{1}H NMR (270 MHz, C$_6$D$_6$): δ 0.16 (9H, s, (CH_3)$_3$Si), 1.86 (2H, m, J_{H-H} = 7 Hz, CH$_2$CH_2CH$_2$), 2.21 (2H, m, J_{H-H} = 6.9 Hz, PCH_2), 3.70 (2H, t, J_{H-H} = 6.4 Hz, OCH_2), 7.03, 7.69 (10H, m, P(C$_6$H$_5$)$_2$). ^{31}P{^{1}H} NMR (270 MHz, C$_6$D$_6$): δ 27.2 (d, J_{Rh-P} = 121 Hz). IR (Nujol): ν_{CO} 2080, 2010 cm^{-1}. Anal. Calcd for C$_{20}$H$_{25}$O$_3$PClSiRh (510.82): 47.03; H, 4.93. Found: C, 48.12; H, 4.98. ^{31}P{^{1}H} NMR (cross polarization): δ 24.9 (d). XPS (Al Kα): Si (2p, 97 eV), P (2s, 193 eV), C (1s, 280 eV), O (1s, 527 eV), Cl (2s, 264 eV), Rh (3d, 308 eV).

[(CH₃)₃SiN(C₂H₅)₂]RhCl(P(C₆H₅)₃)₂ (14). RhCl(P(C₆H₅)₃)₃ (60 mg, 0.065 mmol) was dissolved in 20 mL of benzene, to which 12.2 μL (0.065 mmol) of (CH₃)₃SiN(C₂H₅)₂ was added. The mixture was left to react at room temperature for 24 h, followed by 5 h at 65 °C, which resulted in a color change from deep red to orange. The solvent was evaporated to dryness under vacuum, and the orange residue was washed with diethyl ether followed by recrystallization from a toluene/hexane mixture to afford an orange powder. Yield: 45 mg (86.5%). ¹H NMR (270 MHz, CDCl₃): δ 0.19 (9H, s, (CH_3)₃Si), 1.11 (6H, t, J_{H-H} = 6.9 Hz, NCH₂CH_3), 3.27 (4H, q, J_{H-H} = 7.2 Hz, NCH_2CH₃), 7.02, 7.75 (30H, m, P(C₆H_5)₃). ³¹P{¹H} NMR (270 MHz, CDCl₃): δ 54.5 (d, J_{Rh-P} = 195 Hz). FAB-MS: m/z 809. Anal. Calcd for C₄₃H₄₉P₂NClSiRh (808.26): C, 63.89; H, 6.11; N, 1.73. Found: C, 63.06; H, 6.05; N, 1.80. ³¹P{¹H} NMR (cross polarization): δ 56.2 (d). XPS (Al Kα): Si (2p, 97 eV), P (2s, 193 eV), C (1s, 280 eV), O (1s, 528 eV), N (2s, 395 eV), Cl (2s, 264 eV), Rh (3d, 309 eV).

[(CH₃)₃SiO(CH₂)₃N(C₂H₅)₂]RhCl(CO)(P(C₆H₅)₃) (15). RhCl(CO)(P(C₆H₅)₃)₂ (35 mg, 0.051 mmol) and compound **2** (10.3 μL, 0.051 mmol) were dissolved in 20 mL of benzene. The mixture was refluxed at 70 °C for 5 h under a stream of nitrogen, resulting in a color change from yellow to red. The solvent was removed in vacuo, affording a red solid that was recrystallized from a toluene/hexane mixture. Yield: 22 mg (69%). ¹H NMR (270 MHz, C₆D₆): δ 0.11 (9H, s, (CH_3)₃Si), 0.94 (6H, t, J_{H-H} = 7.2 Hz, NCH₂CH_3), 1.71 (2H, t, J_{H-H} = 7.2 Hz, NCH_2CH₂), 2.19 (2H, m, J_{H-H} = 7.2 Hz, CH₂CH_2CH₂), 2.27 (4H, q, J_{H-H} = 6 Hz, NCH_2CH₃), 3.79 (2H, t, J_{H-H} = 6 Hz, OCH_2), 7.02, 7.92 (15H, m, P(C₆H_5)₃). ³¹P{¹H} NMR (270 MHz, C₆D₆): δ 46.7 (d, J_{Rh-P} = 174 Hz). IR (C₆H₆): ν_{CO} 1968 cm⁻¹. FAB-MS: m/z 632. Anal. Calcd for C₂₉H₄₀O₂PClNSiRh (632.06): C, 55.11; H, 6.38; N, 2.22. Found: C, 55.32; H, 6.26; N, 2.23.

[(CH₃)₃SiOCH(CH₃)(CH₂)₃N(C₂H₅)₂]RhCl(CO)(P-(C₆H₅)₃) (16). A solution of RhCl(CO)(P(C₆H₅)₃)₂ (40 mg, 0.058 mmol) in 30 mL of benzene and compound **3** (13.4 μL, 0.058 mmol) was allowed to reflux at 70 °C for 18 h, resulting in a color change from yellow to orange. Solvent was removed in vacuo, resulting in an orange residue, which was recrystallized from a toluene/hexane mixture affording an orange powder. Yield: 24 mg (63%). ¹H NMR (270 MHz, C₆D₆): δ 0.14 (9H, s, (CH_3)₃Si), 0.98 (6H, t, J_{H-H} = 7.2 Hz, NCH₂CH_3), 1.26 (3H, d, J_{H-H} = 6.2 Hz, CH(CH_3)), 1.42 (2H, m, J_{H-H} = 5.4 Hz, CH₂CH_2-CH₂), 1.57 (2H, q, J_{H-H} = 5.4 Hz, CH_2CH(CH₃)), 2.32 (4H, q, J_{H-H} = 5.4 Hz, NCH_2CH₃), 2.42 (2H, t, J_{H-H} = 5.7 Hz, NCH_2-CH₂), 3.74 (1H, m, J_{H-H} = 5.9 Hz, CH(CH₃)), 6.98, 7.96 (15 H, m, P(C₆H_5)₃). ³¹P{¹H} NMR (270 MHz, C₆D₆): δ 46.4 (d, J_{Rh-P} = 158 Hz). IR (C₆H₆): ν_{CO} 1961 cm⁻¹. FAB-MS: m/z 661. Anal. Calcd for C₃₁H₄₄O₂PNClSiRh (660.11): C, 56.40; H, 6.72; N, 2.12. Found: C, 56.21; H, 6.65; N, 2.16. ³¹P{¹H} NMR (cross polarization): δ 43.0 (d). XPS (Al Kα): Si (2p, 97 eV), P (2s, 193 eV), C (1s, 280 eV), O (1s, 528 eV), N (2s, 395 eV), Cl (2s, 267 eV), Rh (3d, 312 eV).

[(CH₃)₃SiOC₆H₄N(C₂H₅)₂]RhCl(CO)(P(C₆H₅)₃) (17). RhCl-(CO)(P(C₆H₅)₃)₂ (25 mg, 0.036 mmol) and compound **1** (8.62 μL, 0.036 mmol) were dissolved in benzene (20 mL) and allowed to reflux at 70 °C for 15 h. The solvent was then removed in vacuo, and recrystallization from a toluene/hexane mixture yielded an orange solid. Yield: 0.022 g (89.6%). ¹H NMR (270 MHz, C₆D₆): δ 0.14 (9H, s, (CH_3)₃Si), 0.92 (6H, t, J_{H-H} = 7.2 Hz, NCH₂CH_3), 3.02 (4H, q, J_{H-H} = 7.2 Hz, NCH_2-CH₃), 6.32, 6.43, 7.12 (4H, m, C₆H_4N), 7.09, 7.70 (15H, m, P(C₆H_5)₃). ³¹P{¹H} NMR (270 MHz, C₆D₆): δ 47.9 (d, J_{Rh-P} = 177 Hz). IR (C₆H₆): ν_{CO} 1964 cm⁻¹. FAB-MS: m/z 667. Anal. Calcd for C₃₂H₃₈O₂PNClSiRh (666.08): C, 57.70; H, 5.75; N, 2.10. Found: C, 57.06; H, 5.46; N, 2.24.

[(CH₃)₃SiO(CH₂)₃P(C₆H₅)₂]Pd(P(C₆H₅)₃)₃ (18). Pd(P-(C₆H₅)₃)₄ (50 mg, 0.043 mmol) was dissloved in 30 mL of THF, to which compound **5** (13.7 μL 0.043 mmol) was added, and the mixture was refluxed at 75 °C for 20 h. The solution was

concentrated to 5 mL and layered with 15 mL of diethyl ether. A pale yellow microcrystalline solid that precipitated was filtered in vacuo, washed with diethyl ether, and dried under vacuum. Yield: 47.5 mg (91%). ¹H NMR (270 MHz, C₆D₆): δ 0.04 (9H, s, (CH_3)₃Si), 1.75 (2H, m, J_{H-H} = 6 Hz, CH₂CH_2CH₂), 2.13 (2H, m, J_{H-H} = 6 Hz, PCH_2), 3.38 (2H, t, J_{H-H} = 5 Hz, OCH_2), 6.97, 7.48, (10H, m, P(C₆H_5)₂), 7.02, 7.78 (45H, m, P(C₆H_5)₃). ³¹P{¹H} NMR (270 MHz, C₆D₆): δ 13.72 (br, s). FAB-MS: m/z 1208. Anal. Calcd for C₇₂H₇₀P₄OSiPd (1209.75): C, 71.48; H, 5.83. Found: C, 71.35; H, 5.76. XPS (Al Kα): Si (2p, 98 eV), P (2s, 188 eV), C (1s, 280 eV), O (1s, 528 eV), Pd (3d, 337 eV).

[(CH₃)₃SiO(CH₂)₃P(C₆H₅)₂]RuCl₂(CO)₂(P(C₆H₅)₃) (19). A mixture of RuCl₂(CO)₂(P(C₆H₅)₃)₂ (200 mg, 0.27 mmol) and compound **5** (84 μL, 0.27 mmol) in 30 mL of THF was set to reflux at 70 °C for 20 h. The solution was concentrated to 10 mL and layered with hexane (20 mL). A white crystalline solid was filtered, washed with hexanes, and dried in vacuo. Yield: 185 mg (88.5%). ¹H NMR (270 MHz, C₆D₆): δ 0.05 (9H, s, (CH_3)₃Si), 1.89 (2H, m, J_{H-H} = 6.2 Hz, CH₂CH_2CH₂), 2.17 (2H, m, J_{H-H} = 6.2 Hz, PCH_2), 3.57 (2H, t, J_{H-H} = 6 Hz, OCH_2), 7.02, 7.38 (10H, m, P(C₆H_5)₂), 7.75, 8.22 (15H, m, P(C₆H_5)₃). ³¹P{¹H} NMR (270 MHz, C₆D₆): δ 20.5, 19.2 ppm. IR (Nujol): ν_{CO} 2062, 1982 cm⁻¹ FAB-MS: m/z 806. Anal. Calcd for C₃₈H₄₀P₂O₃Cl₂SiRu (806.73): C, 56.57; H, 4.99. Found: C, 56.58; H, 4.53. ³¹P{¹H} NMR (cross polarization): δ 19.8, 17.0 (s). XPS (Al Kα): Si (2p, 98 eV), P (2s, 197 eV), C (1s, 280 eV), O (1s, 529 eV), Cl (2s, 271 eV), Ru (3p, 482 eV).

Surface Reactions and Characterization. General Procedure. Clean substrates of glass, quartz, single-crystal silicon, and ground glass silica were first treated with a toluene solution of SiCl₄ (10% v/v) at room temperature for 18 h. They were then washed with copious amounts of dry toluene, placed in a solution of fresh toluene containing 5% v/v HN(C₂H₅)₂, and left to stir at 70 °C for 14 h. The substrates were washed with toluene, then immersed in a toluene solution containing appropriate ligands, and left to react at room temperature for 24 h. They were washed with toluene and dried under a stream of nitrogen. The ligands deposited on silica and flat glass surfaces include: HO−C₆H₄PPh₂ (**20**), HO−(CH₂)₃PPh₂ (**21**), HO−(CH₂)₄PEt₂ (**22**), HO−C₆H₄NEt₂ (**23**), HO−(CH₂)₃-NEt₂ (**24**), and HO−CH(CH₃)(CH₂)₃NEt₂ (**25**). Solid-state ³¹P-{¹H} CP/MAS experiments were performed on functionalized ground glass silica, and the contact angle measurements were carried out on flat glass surfaces.

[Si]−O−C₆H₄-P(C₆H₅)₂ (20). Solid-state ³¹P{¹H} NMR (cross polarization with xmtr blanking): δ 26.7 ppm. Contact angles: θ_{H_2O} = 91°; $\theta_{Hexadecane}$ = 8°.

[Si]−O−(CH₂)₃P(C₆H₅)₂ (21). Solid-state ³¹P{¹H} NMR (cross polarization with xmtr blanking): δ −16.01 ppm. Contact angles: θ_{H_2O} = 94°; $\theta_{Hexadecane}$ = 7°.

[Si]−O−(CH₂)₄P(C₂H₅)₂ (22). Solid-state ³¹P{¹H} NMR (cross polarization with xmtr blanking): δ −23.2 ppm. Contact angles: θ_{H_2O} = 96°; $\theta_{Hexadecane}$ = 7°.

[Si]−O−C₆H₄N(C₂H₅)₂ (23). Contact angles: θ_{H_2O} = 68°; $\theta_{Hexadecane}$ = 15°.

[Si]−O−(CH₂)₃N(C₂H₅)₂ (24). Contact angles: θ_{H_2O} = 73°; $\theta_{Hexadecane}$ = 12°.

[Si]−O−CH(CH₃)(CH₂)₃N(C₂H₅)₂ (25). Contact angles: θ_{H_2O} = 74°; $\theta_{Hexadecane}$ = 12°.

Organometallic Thin Films. A general procedure for functionalizing inorganic oxide surfaces such as ground glass silica, glass, quartz, and single-crystal silicon with transition-metal complexes is described below.

Ground Glass Silica: **[Si]−O−(CH₂)₃P(C₆H₅)₂Ni(CO)₂-(P(C₆H₅)₃) (26a).** Ni(CO)₂(P(C₆H₅)₃)₂ (250 mg) was dissolved in 50 mL of toluene. Ground glass silica functionalized with **22** was added, and the mixture was set to reflux at 90 °C for 24 h. It was then filtered and washed with copious amounts of toluene and dried in vacuo, resulting in the formation of the surface-anchored complex **26a**.

Flat Glass/Quartz/Single-Crystal Si (26b). Ni(CO)$_2$-(P(C$_6$H$_5$)$_3$)$_2$ (25−50 mg) was dissolved in 30 mL of toluene in a self-assembly apparatus containing a glass slide functionalized with **21** positioned in a Teflon carrousel. The solution was refluxed at 90 °C for 24 h, followed by washing of the glass slide with toluene (3 × 30 mL) and drying under a nitrogen atmosphere.

[26a,b]. Solid state ^{31}P{^{1}H} NMR (cross polarization via spinlock): δ 29.5 (br s). FT-IR (KBr): ν_{CO} 1998, 1934 cm^{-1}. FT-IR-ATR (KRS): ν_{CO} 1996, 1935, cm^{-1}. XPS (Al Kα): Si (2p, 102.6 eV), P (2s, 199 eV), C (1s, 284.9 eV), O (1s, 532 eV), Ni (2p, 859.0 eV). UV−vis (quartz): monolayer coverage 3 × 10^{-9} mol/cm^2.

[Si]−O−(CH$_2$)$_4$P(C$_2$H$_5$)$_2$Ni(CO)$_2$(P(C$_6$H$_5$)$_3$) (27). Solid-state ^{31}P{^{1}H} NMR (single pulse with decoupling xmtr blanking): δ 28.1, 28.8 ppm. FT-IR (KBr): ν_{CO} 1996, 1932 cm^{-1}. XPS (Al Kα): Si (2p, 102.5 eV), P (2s, 198.2 eV), C (1s, 287 eV), O (1s, 530.2 eV), Ni (2p, 858.0 eV).

[Si]−N(C$_2$H$_5$)$_2$Ni(CO)$_2$(P(C$_6$H$_5$)$_3$) (28). Solid-state ^{31}P{^{1}H} NMR (cross polarization via spinlock): δ 31.2 ppm. FT-IR (KBr): ν_{CO} 1980, 1936 cm^{-1}. XPS (Al Kα): Si (2p, 105.9 eV), P (2s, 199.5 eV), C (1s, 286.2 eV), N (1s, 401.5 eV), O (1s, 531 eV), Ni (2p, 858.0 eV).

[Si]−O−(CH$_2$)$_2$N(C$_2$H$_5$)$_2$Ni(CO)$_2$(P(C$_6$H$_5$)$_3$) (29). Solid-state ^{31}P{^{1}H} NMR (cross polarization with transmitter blanking): δ 28.8 ppm. FT-IR (KBr): ν_{CO} 1982, 1935 cm^{-1}. XPS (Al Kα): Si (2p, 109.3 eV), P (2s, 203.5 eV), C (1s, 288.2 eV), N (1s, 400.7 eV), O (1s, 531.6 eV), Ni (2p, 856.0 eV).

[Si]−O−CH(CH$_3$)(CH$_2$)$_3$N(C$_2$H$_5$)$_2$Ni(CO)$_2$(P(C$_6$H$_5$)$_3$) (30). Solid-state ^{31}P{^{1}H} NMR (cross polarization with transmitter blanking): δ 28.4 ppm. FT-IR (KBr): ν_{CO} 1975, 1911 cm^{-1}. XPS (Al Kα): Si (2p, 106.6 eV), P (2s, 200.6 eV), C (1s, 286.9 eV), N (1s, 400.2 eV), O (1s, 530.9 eV), Ni (2p, 856.0 eV).

[Si]−O−(CH$_2$)$_3$P(C$_6$H$_5$)$_2$Rh(CO)$_2$Cl (31). [Rh(CO)$_2$Cl]$_2$ (25 mg) and the substrates functionalized with **21** in toluene were stirred for 4 h at ambient temperature to afford (**31**). Solid-state ^{31}P{^{1}H} NMR (cross polarization with transmitter blanking): δ 23.4 (d, J_{Rh-P} = 93 Hz). FT-IR (KBr): ν_{CO} 2079, 2001 cm^{-1}. XPS (Al Kα): Si (2p, 103.4 eV), P (2s, 198.2 eV), C (1s, 285.1 eV), Cl (2s, 269.6 eV), O (1s, 531.7 eV), Rh (3d, 310.4 eV).

[Si]−O−(CH$_2$)$_3$P(C$_6$H$_5$)$_2$RhCl(CO)(P(C$_6$H$_5$)$_3$) (32). RhCO-(Cl)(P(C$_6$H$_5$)$_3$)$_2$ (25 mg) dissolved in toluene and the susbstrates functionalized with **21** were stirred at 50 °C for 20 h to give a thin film of (**32**). Solid-state ^{31}P{^{1}H} NMR (cross polarization with transmitter blanking): δ 28.1 (d, J_{Rh-P} = 132 Hz), 31.5 (t, J_{P-P} = 366 Hz), 34.9 (d, J_{Rh-P} = 132 Hz). FT-IR (KBr): ν_{CO} 1964 cm^{-1}. FT-IR-ATR (KRS): ν_{CO} = 1964 cm^{-1}. XPS (Al Kα): Si (2p, 103.7 eV), P (2s, 199.8 eV), C (1s, 284.9 eV), Cl (2s, 269.2 eV), O (1s, 530.8 eV), Rh (3d, 307.7 eV).

[Si]−N(C$_2$H$_5$)$_2$RhCl(P(C$_6$H$_5$)$_3$)$_2$ (33). RhCl(P(C$_6$H$_5$)$_3$)$_3$ (25 mg) dissolved in benzene and the substrates functionalized with diethylamine were left to stir at ambient temperature for 24 h, followed by refluxing at 65 °C for 5 h to result in the formation of a thin film of **33**. Solid-state ^{31}P{^{1}H} NMR (cross polarization with transmitter blanking): δ 51.1 (d, J_{Rh-P} = 185 Hz), 58.3 (d, J_{Rh-P} = 185 Hz). XPS (Al Kα): Si (2p, 109.5 eV), P (2s, 204.6 eV), C (1s, 289.7 eV), N (1s, 401.8 eV), Cl (2s, 270.8 eV), O (1s, 533 eV), Rh (3d, 315.2 eV).

[Si]−O−(CH$_2$)$_2$N(C$_2$H$_5$)$_2$RhCl(CO)(P(C$_6$H$_5$)$_3$) (34). RhCO-(Cl)(P(C$_6$H$_5$)$_3$)$_2$ dissolved in benzene and the substrates functionalized with **24** were stirred at 70 °C for 5 h to afford a thin film of **34**. Solid-state ^{31}P{^{1}H} NMR (cross polarization with transmitter blanking): δ 47.5 (d, J_{Rh-P} = 163 Hz). FT-IR (KBr): ν_{CO} 1958 cm^{-1}. XPS (Al Kα): Si (2p, 103 eV), P (2s, 197.9 eV), C (1s, 285.7 eV), N (1s, 399.5 eV), Cl (2s, 268.7 eV), O (1s, 531 eV), Rh (3d, 310.8 eV).

[Si]−O−CH(CH$_3$)(CH$_2$)$_3$N(C$_2$H$_5$)$_2$RhCl(CO)(P(C$_6$H$_5$)$_3$) (35). RhCO(Cl)(P(C$_6$H$_5$)$_3$)$_2$ dissolved in toluene and the substrates functionalized with **25** were stirred at 70 °C for 18 h to give a thin film of **35**. Solid-state ^{31}P{^{1}H} NMR (cross polarization

with transmitter blanking): δ 48.6 (d, J_{Rh-P} = 164 Hz). FT-IR (KBr): ν_{CO} 1954 cm^{-1}. XPS (Al Kα): Si (2p, 105.5 eV), P (2s, 200.3 eV), C (1s, 286.6 eV), N (1s, 400.1 eV), Cl (2s, 270.9 eV), O (1s, 531.3 eV), Rh (3d, 311.8 eV).

[Si]−O−C$_6$H$_4$−N(C$_2$H$_5$)$_2$RhCl(CO)(P(C$_6$H$_5$)$_3$) (36). The conditions of deposition were similar to that for **35**. Solid-state ^{31}P{^{1}H} NMR (cross polarization with transmitter blanking): δ 47.5 (br). FT-IR (KBr): ν_{CO} 1956 cm^{-1}. XPS (Al Kα): Si (2p, 105.3 eV), P (2s, 200.3 eV), C (1s, 286.4 eV), N (1s, 398.9 eV), Cl (2s, 269.7 eV), O (1s, 531 eV), Rh (3d, 311.6 eV).

[Si]−O−(CH$_2$)$_3$P(C$_6$H$_5$)$_2$Pd(P(C$_6$H$_5$)$_3$)$_3$ (37). Pd(P(C$_6$H$_5$)$_3$)$_4$ (25 mg) dissolved in THF and the substrates functionalized with **21** were refluxed at 75 °C for 20 h to result in the formation of a thin film of **37**. Solid-state ^{31}P{^{1}H} NMR (cross polarization with transmitter blanking): δ 14.6 (br s). XPS (Al Kα): Si (2p, 104.2 eV), P (2s, 195.2 eV), C (1s, 286 eV), O (1s, 534.3 eV), Pd (3d, 338.2 eV).

[Si]−O−(CH$_2$)$_3$P(C$_6$H$_5$)$_2$RuCl$_2$(CO)$_2$P(C$_6$H$_5$)$_3$ (38). The conditions of deposition were similar to that for **37**. Solid-state ^{31}P{^{1}H} NMR (cross polarization with transmitter blanking): δ 17.6 (br s). FT-IR (KBr): ν_{CO} 2054, 1996 cm^{-1}. XPS (Al Kα): Si (2p, 105.3 eV), P (2s, 201.1 eV), C (1s, 287.2 eV), Cl (2s, 271 eV), O (1s, 531 eV), Ru (3p, 489 eV).

Cyclooligomerization of Phenylacetylene Using Ni(CO)$_2$PPh$_3$[(PPh$_2$(CH$_2$)$_3$OSi(CH$_3$)$_3$] in a Catalyst-to-Monomer Ratio of 1:250. General Procedure. Ni(CO)$_2$P-(C$_6$H$_5$)$_3$[P(C$_6$H$_5$)$_2$(CH$_2$)$_3$OSi(CH$_3$)$_3$] (200 mg, 0.29 mmol) was added under a nitrogen atmosphere to 25 mL of C$_6$H$_6$ containing 7.90 mL (7.35 g, 72.5 mmol) of phenylacetylene, and the mixture was set to reflux at 80 °C for 3 h, during which time the solution went from pale yellow to reddish-brown in color. The benzene and unreacted phenylacetylene (185 μL) were distilled from the reaction mixture. The residue was extracted into petroleum ether, and the insoluble portion was filtered and washed with ether (10 mL) and hexanes (10 mL). The orange filtrate was cooled to −20 °C overnight, resulting in the recrystallization of colorless needles. Evaporating the solvent from the orange filtrate, followed by crystallization in diethyl ether, afforded an orange powder. Total yield of three fractions: 5.88 g (79.9%).

1,2,4-Triphenylbenzene. Yield: 5.35 g (91%). ^{1}H NMR (270 MHz, C$_6$D$_6$): δ 7.16 (s), 7.41 (m). IR (KBr): ν 2945, 1839, 1630, 1515, 1219, 805 cm^{-1}. Mp: 101 °C. GC (C$_6$H$_6$): 5.73 min. GC-MS (C$_6$H$_6$): 40.87 min, m/z 306. UV−vis (C$_6$H$_{12}$): λ_{max} 248, 272 (sh) nm.

1,3,5-Triphenylbenzene. Yield: 0.37 g (6.30%). ^{1}H NMR (270 MHz, C$_6$D$_6$): δ 7.77 (s), 7.51 (d), 7.23 (m). IR (KBr): ν 4051, 3056, 1949, 1884, 1758, 1602, 1111, 999, 872 cm^{-1}. Mp: 171 °C. GC (C$_6$H$_6$): 7.81 min. GC-MS (C$_6$H$_6$): 44.34 min, m/z 306. UV−vis (C$_6$H$_{12}$): λ_{max} 250 nm.

1,3,6-Triphenyhex-1-yne-3,5-diene. Yield: 0.16 g (2.72%). ^{1}H NMR (270 MHz, C$_6$D$_6$): δ 8.00, 6.34, 5.88 (s), 7.20 (m). IR (KBr): ν 3024, 1951, 916 cm^{-1}. Mp: 108 °C. GC (C$_6$H$_6$): 3.39 min. GC-MS (C$_6$H$_6$): 29.42 min, m/z 306. UV−vis (C$_6$H$_{12}$): λ_{max} 206, 281 nm.

Cyclooligomerization of Phenylacetylene Using Ni(CO)$_2$PPh$_3$[(PPh$_2$(CH$_2$)$_3$OSi(CH$_3$)$_3$] in a Catalyst-to-Monomer Ratio of 1:24000. General Procedure. Ni(CO)$_2$P-(C$_6$H$_5$)$_3$[P(C$_6$H$_5$)$_2$(CH$_2$)$_3$OSi(CH$_3$)$_3$] (3.8 mg 0.005 mmol) was dissolved in 20 mL of C$_6$H$_6$, to which 14.27 mL of phenylacetylene (13.4 g, 0.131 mol) was added. The reaction mixture was set to reflux at 80 °C for 3 h, followed by distillation of benzene and phenylacetylene. Total yield of three fractions: 0.48 g (3.65%).

1,2,4-Triphenylbenzene. Yield: 0.425 g (87.9%). ^{1}H NMR (270 MHz, C$_6$D$_6$): δ 7.15 (s), 7.48 (m). IR (KBr): ν 2945, 1839, 1653, 1515, 1219, 805 cm^{-1}. Mp: 102 °C. GC (C$_6$H$_6$): 5.687 min. GC-MS (C$_6$H$_6$): 40.75 min, m/z 306. UV−vis (C$_6$H$_{12}$): λ_{max} 249, 272 (sh) nm.

1,3,5-Triphenylbenzene. Yield: 0.025 g (5.18%). ^{1}H NMR (270 MHz, C_6D_6): δ 7.77 (s), 7.51 (d), 7.23 (m). IR (KBr): ν 4051, 3057, 1949, 1884, 1757, 1593, 1111, 998, 872 cm^{-1}. Mp: 172 °C. GC (C_6H_6): 7.459 min. GC-MS (C_6H_6): 44.31 min, m/z 306. UV−vis (C_6H_{12}): λ_{max} 250 nm.

1,3,6-Triphenyhex-1-yne-3,5-diene. Yield: 0.03 g (6.21%). ^{1}H NMR (270 MHz, C_6D_6): δ 8.00, 6.34, 5.88 (s), 7.20 (m). IR (KBr): ν 3031, 2250 (w), 1951, 916 cm^{-1}. Mp: 108 °C. GC (C_6H_6): 3.411 min. GC-MS (C_6H_6): 29.02 min, m/z 306. UV−vis (C_6H_{12}): λ_{max} 206, 281 nm.

Cyclooligomerization of Phenylacetylene Using a Supported Ni(0) Complex: [Si]−O−(CH$_2$)$_3$PPh$_2$Ni(CO)$_2$-PPh$_3$. The catalytic reaction was performed using the Ni(0) complex [Si]-O−(CH$_2$)$_3$P(C$_6$H$_5$)$_2$Ni(CO)$_2$P(C$_6$H$_5$)$_3$ surface-immobilized on a 1 in. × 1 in. glass slide. The slide was placed in a self-assembly apparatus equipped for stirring and heating. Benzene (10 mL) was added to cover the slide, and 100 μL of dry and distilled phenylacetylene was also introduced. The mixture was set to reflux at 90 °C for 4 h, resulting in a color change from colorless to bright yellow. The resulting solution was distilled to remove benzene and excess phenylacetylene, leaving behind an orange-brown oily residue characterized by ^{1}H NMR, FT-IR, UV−vis, melting points, GC, and GC-MS. The percentage of the trimers are based on GC-MS results. Total yield: 0.075 g (80.65%).

1,3,5-Triphenylbenzene. ^{1}H NMR (270 MHz, C_6D_6): δ 7.77 (s), 7.51 (m), 7.23 (m). IR (CH$_2$Cl$_2$): ν 2974, 1602, 1096, 996, 860 cm^{-1}. Mp: 172 °C. GC (C_6H_6): 7.879 min, 58.84%. GC-MS (C_6H_6): 44.71 min, m/z 306, 56.01%. UV−vis (C_6H_{12}): λ_{max} 250 nm.

1,2,4-Triphenylbenzene. ^{1}H NMR (270 MHz, C_6D_6): δ 7.15 (s), 7.24 (m). IR (CH$_2$Cl$_2$): ν 2932 cm^{-1}. Mp: 102 °C. GC (C_6H_6): 5.808 min, 23.13%. GC-MS (C_6H_6): 40.76 min, m/z 306, 20.64%. UV−vis (C_6H_{12}): λ_{max} 250, 272 (sh) nm.

1,4,6-Triphenyhex-1-yne-3,5-diene. ^{1}H NMR (270 MHz, C_6D_6): δ 8.09 (d, J_{H-H} = 16 Hz), 6.82 (d, J_{H-H} = 16 Hz), 5.89 (s), 7.24 (m). IR (CH$_2$Cl$_2$): ν 3024, 1950, 835 cm^{-1}. Mp: 109 °C. GC (C_6H_6): 3.426 min, 18.03%. GC-MS (C_6H_6): 28.75 min, m/z 306, 23.01%. UV−vis (C_6H_{12}): λ_{max} 280 nm.

Mechanistic Studies Using FT-IR. A glass slide containing the supported metal complex [Si]−O−(CH$_2$)$_3$P(C$_6$H$_5$)$_2$Ni-(CO)$_2$PPh$_3$ was placed in benzene in an apparatus equipped with KBr windows. A 100 μL amount of dry and distilled phenylacetylene was added, and the reaction vessel was lowered in an oil bath set at 90 °C. After a period of 15, 30, and 45 min, etc., the reaction vessel was removed from the oil bath. Benzene, phenylacetylene, and any organic products were syringed out, and the glass slide was washed with 2 × 50 mL of benzene followed by drying the glass slide under a stream of nitrogen. The FT-IR spectra of the thin film were taken, and this procedure was repeated after 30, 60, 120, and 240 min. Benzene and unreacted phenylacetylene were distilled under vacuum, leaving behind a yellow residue, which was recrystallized from diethyl ether and characterized by ^{1}H NMR, FT-IR, UV−vis, melting points, GC, and GC-MS.

Quantitative XPS Study of the Thin Films of [Si]−O−(CH$_2$)$_3$PPh$_3$Ni(CO)$_2$PPh$_3$ Before and After Catalysis. Two glass slides (1 in. × 1 in.) were functionalized with the Ni complex, [Si]−O−(CH$_2$)$_3$PPh$_2$Ni(CO)$_2$PPh$_3$, as previously described. One of the slides was removed and used for the quantitative XPS study, and the second slide was subjected to catalytic oligomerization of phenylacetylene. After 4 h, the slide was removed from the self-assembly apparatus, washed copiously with toluene, dried under a stream of nitrogen, and its X-ray photoelectron spectra was recorded. Benzene and unreacted phenylacetylene from the organic portion were distilled under vacuum, leaving behind a yellow residue, which was recrystallized from diethyl ether and characterized by ^{1}H NMR, FT-IR, UV−vis, melting points, GC, and GC-MS.